

Article

Bond Strength of Reinforcing Steel Bars in Self-Consolidating Concrete

Micheal Asaad and George Morcous * 

Durham School of Architectural Engineering and Construction, College of Engineering, University of Nebraska—Lincoln, 1110 South 67th Street, Omaha, NE 68182-0816, USA; micheal.asaad@kiewit.com

* Correspondence: gmorcous2@unl.edu

Abstract: This paper presents an experimental investigation of the bond strength of reinforcing steel bars in tension in self-consolidating concrete (SCC). The effects of the reinforcing bar's location, orientation, size, and coating on the bond strength with SCC were studied and compared to those with conventionally vibrated concrete (CVC). Several SCC mixtures were developed to cover a wide range of applications/components and material types. The fresh properties of the SCC mixtures were determined to evaluate their filling ability, passing ability and stability. Two hundred and thirty-four pull-out tests of rebars embedded in cubes, wall panels and slabs were conducted. Almost half of the tests were conducted to evaluate the bond with SCC and the other half with CVC. Load–slippage relationships were measured for each test. Pull-out test results were analyzed, and the bond strength was reported in two values: critical strength, which corresponds to slippage of 0.01 in. *0.25 mm; and ultimate strength, which corresponds to the maximum load. The critical strength of SCC and CVC were compared against the ACI 318-19 provisions and comparisons between the ultimate strength of SCC and CVC were conducted. The comparisons indicated that SCC has lower bond strength with vertical rebars than CVC, and a 1.3 development length modification factor is recommended. A similar conclusion applies to epoxy-coated and large diameter rebars. Also, SCC with high slump flow has shown a less top-bar effect than that of CVC.

Keywords: bond strength; self-consolidating concrete; top-bar effect; orientation of the rebar; epoxy-coated rebar



Citation: Asaad, M.; Morcous, G. Bond Strength of Reinforcing Steel Bars in Self-Consolidating Concrete. *Buildings* **2023**, *13*, 3009. <https://doi.org/10.3390/buildings13123009>

Academic Editors: Lei Li, Jiantao Wang and Yixin Zhang

Received: 16 October 2023
Revised: 21 November 2023
Accepted: 25 November 2023
Published: 1 December 2023



Copyright: © 2023 by the authors. Licensee MDPI, Basel, Switzerland. This article is an open access article distributed under the terms and conditions of the Creative Commons Attribution (CC BY) license (<https://creativecommons.org/licenses/by/4.0/>).

1. Introduction

According to the American Concrete Institute (ACI), a bond is the shearing stress at the surface of a reinforcing bar, preventing relative movement between the bar and the surrounding concrete when the bar carries tensile force. The bond strength between the concrete and reinforcement steel plays a main role in the structural design of different reinforced concrete elements. The main assumption to design these elements is the composite behavior of the cross section, which is provided when the yield of the rebar happens before any slippage of it from the concrete. To ensure that no slippage happens, all building codes list certain criteria for the development length of rebars in tension. These criteria depend on many factors, such as the yield strength of steel, compressive strength of concrete, weight of concrete (whether it is light or of normal weight), diameter of the rebar, the confining of the reinforcement, location of the rebar, and type of the rebar coating [1]. These criteria do not include the concrete type: conventionally vibrated concrete (CVC) or self-consolidating concrete (SCC). The significant differences between SCC and CVC with respect to aggregate composition, rheology, and use of viscosity modifying admixtures (VMA) are believed to affect the characteristics of the bond with reinforcing bars. The orientation of the bars, whether parallel or perpendicular to the direction of casting, location of bars, bar diameter and coating could also have an influence on the bond strength with SCC different from that with CVC due to differences in composition and rheology of mixtures. Therefore, the

objective of this study is to evaluate the bond strength of reinforcing steel with SCC and compare its behavior with that with CVC when different design parameters are used.

2. Literature Review

Two criteria are used to define the bond strength between concrete and reinforcing steel depending on the purpose of testing. First, the ultimate bond stress, which is the stress at the maximum load. Second, the critical bond stress corresponding to slippage of 0.01 in. (0.25 mm) as proposed by Mathey and Watstein [2], which is more appropriate for design purposes [3]. Pull-out tests are usually used to measure the ultimate and critical bond stresses. Three factors resist the slippage of a rebar in concrete: (1) adhesion between concrete and steel, (2) friction due to rebar confinement, and (3) bearing at bar deformations. Two failure modes are expected: (1) slippage due to shear of the confining concrete [4], (2) splitting in the confining concrete [5].

König et al. [6,7] and Almeida et al. [8] found that CVC performed better in bond tests and achieved 15 to 20% greater bond strength than that of SCC. Almeida et al. [9] evaluated the bond behavior of SCC by varying compressive strength and steel bar diameter in pull-out and beam tests. The comparison between the test results and code equations showed that the same equations adopted for CVC can be used for SCC, which means that bond properties of SCC are similar to those of CVC. Hassan et al. [4] reported that the normalized bond stress was slightly higher in SCC than that in CVC at 3, 7, 14 and 28 days in pull-out tests. Aslani and Nejadi [10] reported that the bond strength of SCC is as high as the bond strength of CVC when large bar diameters are studied. For smaller bar diameters, the bond strength of SCC is slightly higher, with the largest difference occurring for the smallest bar diameters.

Valcuende and Parra [11] conducted pull-out tests and calculated the mean bond strength as the arithmetic mean of the stresses recorded for slips of 0.0004, 0.004 and 0.04 in. (0.01, 0.1, and 1 mm), which was found to be 30% greater in SCC than in 4.5 ksi (31 MPa) CVC, but only 10% greater than in 9 ksi (62 MPa) CVC. The enhanced cohesiveness of SCC ensures a better suspension of solid particles in the fresh state and this, therefore, produces good deformability and filling capability. Bleeding, segregation and surface settlement as a result of a high water-to-cement ratio (w/c) or excessive vibration are generally not factors considered in SCC, which explains the higher bond strength even in deep members [4]. Gibbs and Zhu [12] reported a 4% difference in bond strength between the two types of concrete, Wang and Zheng [13] reported 9%, and Daoud et al. [14] reported 5% higher bond strength for SCC. Zhu et al. [15] reported that the normalized bond strengths of the SCC mixes were found to be about 10–40% higher than those of CVC mixes with the same strength, while the maximum bond strength decreased when the diameter of the steel bar increased from 1/2 to 3/4 in. (13 to 19 mm). Cattaneo and Rosati [5] found SCC exhibits higher bond strength and, compared to CVC, requires a larger concrete cover to attain pull-out failure. Desnerck et al. [16] conducted beam tests to evaluate the bond of reinforcement in SCC and CVC and found that for the same compressive strength, the bond strength of SCC is as high as that of CVC for large bar diameters, or slightly higher than that of CVC for smaller bar diameters. The bar diameters ranged from 1/2 to 1.5 in. (13 to 38 mm).

Most researchers agreed that SCC still shows the top-bar effect, but the extent is lower than or similar to CVC, and for concretes of more than 7 ksi (50 MPa), the differences between SCC and CVC are not significant. Khayat [17] found VMA helped reduce surface settlement related to bleeding and segregating and significantly reduced the top-bar effect. Attiogbe et al. [18] concluded that highly stable SCC mixtures have a level of top-bar effect for deformed bars that is similar to that of 4 to 6 in. (100–150 mm) slump concrete. Chan et al. [3] conjectured that the plastic settlement during the hardening of SCC may still cause the top-bar effect and reported that fewer top-bar effects were found for SCC in the pull-out tests than for CVC. Castel et al. [19] concluded that the bond strength of SCC is not affected by the orientation of the bars. For the top casting surface, the maximum

ultimate bond strengths obtained were approximately 20% higher for SCC than for CVC, regardless of the concrete strength. Hassan et al. [4] reported that the bond stress–slip curve showed similar trends of variation for both SCC and CVC pull-out specimens in the bottom bars. Higher bond stress and stiffness in the top and middle bars were observed in SCC compared to CVC. Trezos et al. [20] found that the top-bar effect seems to be less intense in SCC when stress corresponding to slip of 0.01 in. (0.25 mm) is selected as the bond strength. Esfahani et al. [21] studied the effect of bar position on the bond strengths of reinforcing bars using pull-out tests with top, middle and bottom bars. It was found that the local bond strength of bottom cast bars was almost the same for CVC and SCC, but for the top cast bars, the local bond strength for SCC was about 20% less than that for CVC.

Due to the disagreements in the literature on the bond strength of reinforcing rebars in SCC compared to CVC, an extensive experimental investigation was conducted to study the bond strength when a wide range of SCC materials, proportions, and characteristics are used.

3. Materials and Mixture Proportioning

3.1. Materials

Different types of coarse aggregates and supplementary cementitious materials (SCMs) were used in this study to cover the variance in materials' availability based on location [22]. Portland Cement type I/II was used in developing the mixtures in this study, which is commonly used in construction. Two types of coarse aggregate (i.e., crushed limestone and natural gravel) and natural sand were used for all mixtures. For each aggregate type, three nominal maximum sizes of aggregates, NMSA, 3/4, 1/2, and 3/8 in. (19, 13, and 10 mm), were used to represent the sizes used in different concrete components. The physical properties of the aggregates and their combinations are presented in Table 1. Figure 1 shows the particle size distribution of fine and coarse aggregates.

Table 1. Physical properties of aggregates and combination (1 in. = 25.4 mm, 1 pcf = 16 kg/m³).

Property	Limestone			Gravel			Sand
	3/4 in.	1/2 in.	3/8 in.	3/4 in.	1/2 in.	3/8 in.	
Specific Gravity	2.66	2.66	2.66	2.74	2.68	2.69	2.62
Absorption	1.3%	1.3%	1.3%	1.1%	1.4%	1.4%	0.5%
Sand-to-Aggregate Ratio	0.45	0.47	0.50	0.45	0.47	0.50	N/A
Combined Aggregate Unit Weight (pcf)	117	118	118	127	124	123	N/A
Percent of Voids	29.0	28.4	28.4	23.7	25.9	27.0	N/A

In addition to Portland Cement type I/II, three types of SCMs (i.e., Class C fly ash, Class F fly ash, and GGBFS), and one filler (i.e., limestone powder) were used. The chemical compositions of cement, SCMs, and filler are listed in Table 2. The particle size distribution of cement, SCMs, and filler are presented in Figure 2. Chemical admixtures were used to control the rheological properties and durability of SCC mixtures, which include a polycarboxylate-type high-range water-reducing admixture (HRWRA) that meets the requirements of the ASTM C494 type F admixture; a viscosity-modifying admixture (VMA) and workability-retaining admixture that meets the requirements of ASTM C494 type S admixture; and an air-entraining admixture (AEA) that meets the requirements of ASTM C260.

3.2. Proportioning

Proportioning SCC mixtures is different from proportioning CVC mixtures as workability targets, in contrast to compressive strength, usually control the proportioning of the mixture. Workability targets were identified based on the geometric characteristics of the component and production and placement conditions. The geometric characteristics of a

component include the length, depth, thickness, shape intricacy, formed surface quality, and level of reinforcement (i.e., intensity and spacing). Production and placement conditions include mixing energy, transport time, placement technique, and temperature. For simplicity, each of the geometric characteristics was classified as either “high” or “low” [22].

Table 3 shows the value/definition used to describe the classes of each geometric characteristic based on the literature [23,24]. Similarly, two classes were used to describe each of the three key workability properties of SCC: filling ability (FA), segregation resistance (SR), and passing ability (PA). Table 4 shows the value/range of the parameters used to describe the two classes of each workability property based on the literature [23–26]. These values/ranges might be adjusted according to the production and placement conditions [27]. To determine which workability target value/range applies to a specific component, the decision tree shown in Figure 3 is used. This decision tree provides guidelines on workability targets based on the geometric characteristics of the concrete component. The three-digit identification shown at the bottom of the tree represents the target workability with respect to filling ability, segregation resistance, and passing ability classes, respectively. For example, 111 means FA1, SR1, and PA1.

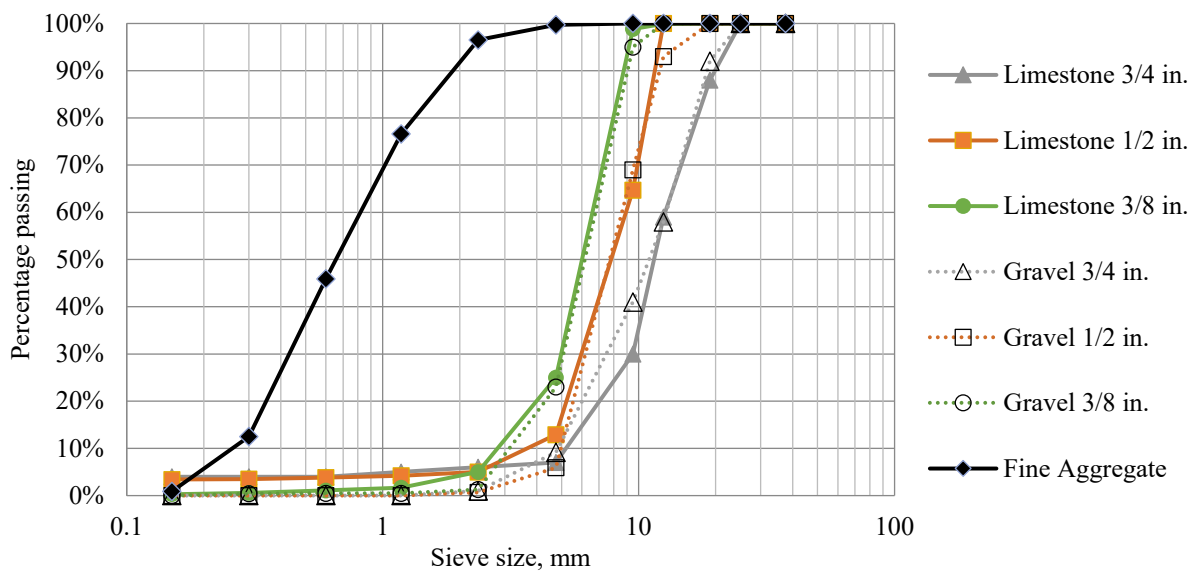


Figure 1. Particle size distribution of fine and coarse aggregates.

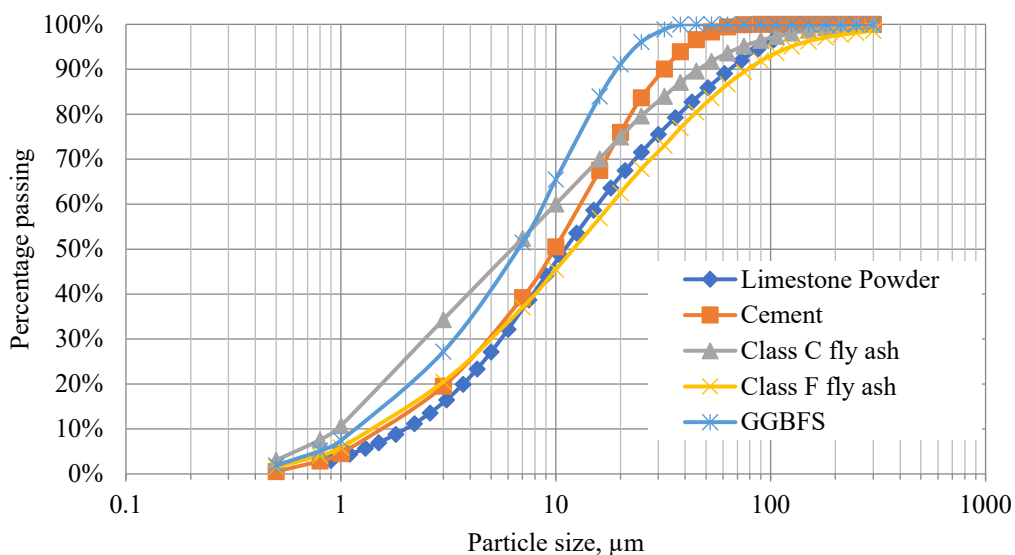


Figure 2. Particle size distribution of cement, SCMs, and filler.

Table 2. Chemical compositions of cement, SCMs and filler.

Component	Component Content by Percentage of Weight				
	Type I/II Cement	Class C Fly Ash	Class F Fly Ash	GGBFS	Limestone Powder
SiO ₂	20.10	42.46	50.87	31.63	1.56
Al ₂ O ₃	4.44	19.46	20.17	11.30	-
Fe ₂ O ₃	3.09	5.51	5.27	0.34	0.48
SO ₃	3.18	1.20	0.61	3.30	1.77
CaO	62.94	21.54	15.78	41.31	52.77
MgO	2.88	4.67	3.19	10.77	0.48
Na ₂ O	0.10	1.42	0.69	0.19	0.03
K ₂ O	0.61	0.68	1.09	0.36	0.09
P ₂ O ₅	0.06	0.84	0.44	0.02	-
TiO ₂	0.24	1.48	1.29	0.56	-
SrO	0.09	0.32	0.35	0.04	-
BaO	-	0.67	0.35	-	-
LOI	2.22	0.19	0.07	-	42.50

Table 3. Classes of component geometric characteristics (1 in. = 25.4 mm, 1 ft = 0.305 m).

Component Geometric Characteristics	Class	Value/Definition
Length	Low	≤33 ft
	High	>33 ft
Depth	Low	≤16 ft
	High	>16 ft
Thickness	Low	≤8 in.
	High	>8 in.
Shape Intricacy	Low	Concrete flows in a single direction
	High	Concrete flow around corners and cutouts
Formed Surface Quality	Low	Unexposed to the travelling public
	High	Exposed to the travelling public
Level of Reinforcement	Low	Large spacing between bars (≥3 in.)
	High	Small spacing between bars (<3 in.)

Several approaches for proportioning SCC mixtures were reviewed and evaluated [25, 27–32]. The procedure proposed by Koehler and Fowler [31] was chosen because it considers the effect of aggregate gradation, shape, and angularity, and uses standard workability test methods to identify the necessary parameters [33]. Two steps were added to the procedure to provide guidance on the water content requirements for different NMSA according to ACI 211 [34], and to verify that powder content and aggregate volume are within the recommended ranges of ACI 237 [25]. Forty normal-weight SCC mixtures containing two types of coarse aggregate (i.e., crushed limestone and natural gravel) with three NMSA, three types of SCMs (i.e., Class C fly ash, Class F fly ash, and GGBFS), and one filler (i.e., limestone powder) were designed to be used in the experimental investigation. Six normal-weight CVC mixtures were proportioned according to ACI 211 [34] procedures for the two types of coarse aggregate with three gradations each (No. 67, No. 79, and No. 8) for comparison, as shown in Tables 5 and 6 [22].

Table 4. Classes of SCC workability properties (1 in. = 25.4 mm).

Workability Property	Class	Value/Range	Application
Filling Ability (FA)	FA1	22 in. \leq Slump Flow $<$ 26 in.	Simple sections
	FA2	26 in. \leq Slump Flow \leq 30 in.	Complex sections or high formed surface quality
Passing Ability (PA)	PA1	80% $>$ Filling Capacity \geq 70% 2 in. $<$ J-Ring $\Delta D \leq$ 4 in. 0.6 in. $<$ J-Ring $\Delta H \leq$ 0.8 in.	Wide spacing between reinforcing bars
	PA2	Filling Capacity \geq 80% J-Ring $\Delta D \leq$ 2 in. J-Ring $\Delta H \leq$ 0.6 in.	Narrow spacing between reinforcing bars
Segregation Resistance (SR)	SR1	10% $<$ Column Segregation \leq 15% 0.5 in. $<$ Penetration \leq 1 in. VSI = 1	Short or shallow components
	SR2	Column Segregation \leq 10% Penetration \leq 0.5 in. VSI = 0	Long or deep components

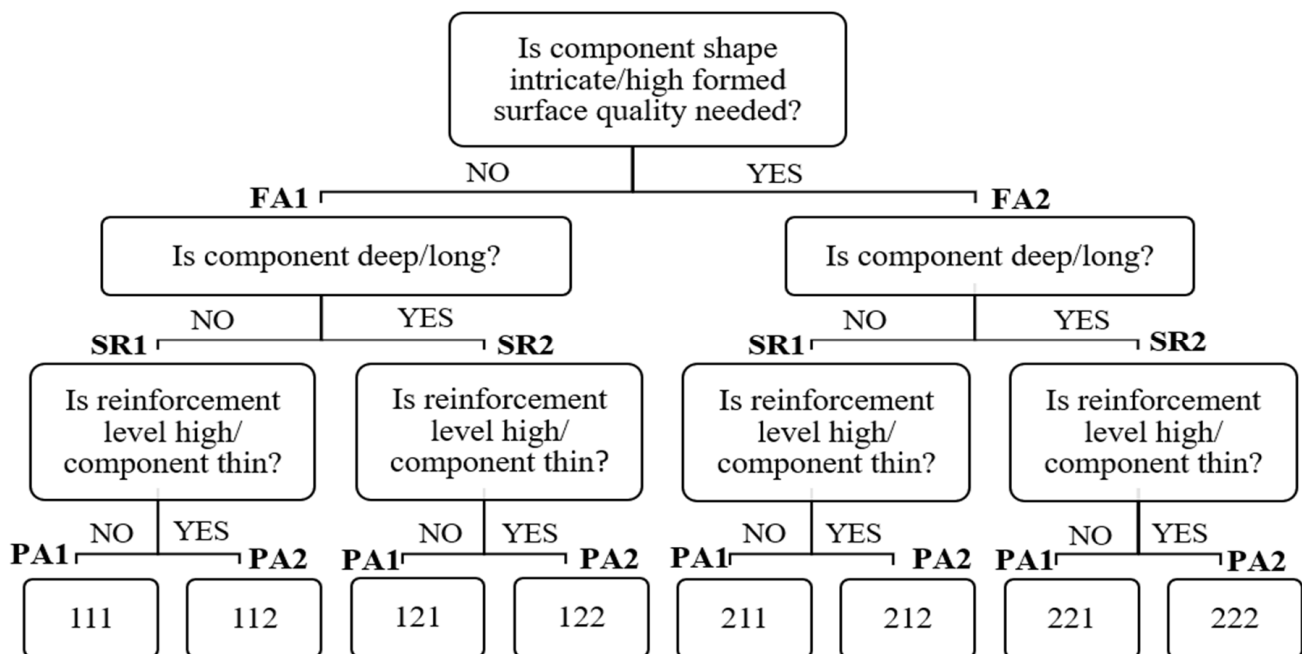
**Figure 3.** Decision tree used to determine workability targets.

Table 5. Proportions of SCC and CVC mixtures containing limestone aggregate.

Mixture Type	SCC Mixtures																				CVC Mixtures		
SCMs/Fillers	25% Class C Fly Ash					25% Class F Fly Ash					30% GGBFS					20% Class F Fly Ash + 15% LSP					25% Class F Fly Ash		
Flowability	Low Slump Flow		High Slump Flow			Low Slump Flow		High Slump Flow			Low Slump Flow		High Slump Flow			Low Slump Flow		High Slump Flow			2–4 in. Slump		
NMSA, in.	3/4	1/2	3/4	1/2	3/8	3/4	1/2	3/4	1/2	3/8	3/4	1/2	3/4	1/2	3/8	3/4	1/2	3/4	1/2	3/8	3/4	1/2	3/8
Mixture ID	111	121	211	221	222	111	121	211	221	222	111	121	211	221	222	111	121	211	221	222	No. 67	No. 78	No. 8
Cement Type I/II, lb/cy	531	535	568	572	587	531	535	568	572	587	521	525	539	543	558	456	460	488	491	504	494	553	572
SCM, lb/cy	177	178	189	191	196	177	178	189	191	196	223	225	231	233	239	140	141	150	151	155	165	184	191
Filler, lb/cy	0	0	0	0	0	0	0	0	0	0	0	0	0	0	0	105	106	113	113	116	0	0	0
Coarse Agg., lb/cy	1542	1462	1518	1439	1334	1542	1462	1518	1439	1334	1542	1462	1530	1450	1345	1542	1462	1518	1439	1334	1674	1485	1350
Natural Sand, lb/cy	1262	1297	1242	1276	1334	1262	1297	1242	1276	1334	1262	1297	1252	1286	1345	1262	1297	1242	1276	1334	1193	1271	1356
Water, lb/cy	280	295	280	295	305	280	295	280	295	305	280	295	280	295	305	280	295	280	295	305	280	295	305
HRWRA, oz/cwt	12.0	14.0	12.0	16.0	13.0	6.0	4.0	8.0	8.0	13.0	12.0	10.0	18.0	16.0	15.0	11.0	9.0	12.0	12.0	15.0	0.0	0.0	0.0
VMA, oz/cwt	0.0	0.0	6.0	0.0	0.0	3.0	0.0	3.0	6.0	0.0	0.0	0.0	3.0	3.0	0.0	0.0	0.0	3.0	6.0	0.0	0.0	0.0	0.0
AEA, oz/cwt	1.5	1.5	1.5	1.5	1.5	1.5	1.5	1.5	1.5	1.5	1.5	1.5	1.5	1.5	1.5	1.5	1.5	1.5	1.5	1.5	1.5	1.5	1.5
Total Weight, lb/cy	3792	3767	3797	3772	3756	3792	3767	3797	3772	3756	3828	3803	3832	3807	3792	3786	3761	3790	3765	3749	3806	3788	3774
Total Aggregate, lb/cy	2804	2759	2760	2714	2669	2804	2759	2760	2714	2669	2804	2759	2782	2737	2691	2804	2759	2760	2714	2669	2867	2756	2706
Total Powder, lb/cy	708	713	757	763	783	708	713	757	763	783	744	750	770	776	797	702	707	751	756	776	659	738	763
W/P Ratio	0.40	0.41	0.37	0.39	0.39	0.40	0.41	0.37	0.39	0.39	0.38	0.39	0.36	0.38	0.38	0.40	0.42	0.37	0.39	0.39	0.43	0.40	0.40
S/A Ratio	0.45	0.47	0.45	0.47	0.50	0.45	0.47	0.45	0.47	0.50	0.45	0.47	0.45	0.47	0.50	0.45	0.47	0.45	0.47	0.50	0.42	0.46	0.50
Paste Volume %	37.0%	38.0%	38.0%	39.0%	40.0%	37.0%	38.0%	38.0%	39.0%	40.0%	37.0%	38.0%	37.5%	38.5%	39.5%	37.0%	38.0%	38.0%	39.0%	40.0%	36.0%	38.5%	39.6%
Coarse Agg. Vol. %	34.4%	32.6%	33.9%	32.1%	29.8%	34.4%	32.6%	33.9%	32.1%	29.8%	34.4%	32.6%	34.1%	32.4%	30.0%	34.4%	32.6%	33.9%	32.1%	29.8%	37.4%	33.1%	30.1%

Table 6. Proportions of SCC and CVC mixtures containing gravel aggregate.

Mixture Type	SCC Mixtures																				CVC Mixtures		
	25% Class C Fly Ash					25% Class F Fly Ash					30% GGBFS					20% Class F Fly Ash + 15% LSP					25% Class F Fly Ash		
SCMs/Fillers	Low Slump Flow		High Slump Flow			Low Slump Flow		High Slump Flow			Low Slump Flow		High Slump Flow			Low Slump Flow		High Slump Flow			2–4 in. Slump		
NMSA, in.	3/4	1/2	3/4	1/2	3/8	3/4	1/2	3/4	1/2	3/8	3/4	1/2	3/4	1/2	3/8	3/4	1/2	3/4	1/2	3/8	3/4	1/2	3/8
Mixture ID	111	121	211	221	222	111	121	211	221	222	111	121	211	221	222	111	121	211	221	222	No. 67	No. 78	No. 8
Cement Type I/II, lb/cy	494	498	568	572	587	494	498	568	572	587	485	489	539	543	558	440	444	488	491	504	459	516	534
SCM, lb/cy	165	166	189	191	196	165	166	189	191	196	208	209	231	233	239	135	137	150	151	155	153	172	178
Filler, lb/cy	0	0	0	0	0	0	0	0	0	0	0	0	0	0	0	102	102	113	113	116	0	0	0
Coarse Agg., lb/cy	1580	1497	1530	1450	1344	1580	1497	1530	1450	1344	1580	1497	1543	1462	1355	1567	1486	1530	1450	1344	1674	1485	1350
Natural Sand, lb/cy	1292	1328	1252	1286	1344	1292	1328	1252	1286	1344	1292	1328	1262	1296	1355	1282	1317	1252	1286	1344	1277	1358	1455
Water, lb/cy	280	295	280	295	305	280	295	280	295	305	280	295	280	295	305	280	295	280	295	305	260	275	285
HRWRA, oz/cwt	5.0	5.0	9.0	5.0	8.0	7.0	4.0	7.0	5.0	5.5	6.0	5.0	10.0	7.0	7.5	3.0	3.0	6.0	7.5	6.0	0.0	0.0	0.0
VMA, oz/cwt	0.0	0.0	3.0	0.0	3.0	0.0	0.0	2.0	3.0	3.0	0.0	0.0	3.0	0.0	0.0	0.0	0.0	2.0	3.0	0.0	0.0	0.0	0.0
AEA, oz/cwt	1.5	1.5	1.5	1.5	1.5	1.5	1.5	1.5	1.5	1.5	1.5	1.5	1.5	1.5	1.5	1.5	1.5	1.5	1.5	1.5	1.5	1.5	1.5
Total Weight, lb/cy	3811	3784	3819	3793	3776	3811	3784	3819	3793	3776	3844	3818	3854	3829	3812	3807	3781	3813	3787	3769	3823	3806	3803
Total Aggregate, lb/cy	2872	2825	2782	2736	2688	2872	2825	2782	2736	2688	2872	2825	2805	2758	2711	2849	2803	2782	2736	2688	2951	2843	2805
Total Powder, lb/cy	659	664	757	763	783	659	664	757	763	783	692	698	770	776	797	677	683	751	756	776	612	688	713
W/P Ratio	0.43	0.44	0.37	0.39	0.39	0.43	0.44	0.37	0.39	0.39	0.40	0.42	0.36	0.38	0.38	0.41	0.43	0.37	0.39	0.39	0.43	0.40	0.40
S/A Ratio	0.45	0.47	0.45	0.47	0.50	0.45	0.47	0.45	0.47	0.50	0.45	0.47	0.45	0.47	0.50	0.45	0.47	0.45	0.47	0.50	0.43	0.48	0.52
Paste Volume %	36.0%	37.0%	38.0%	39.0%	40.0%	36.0%	37.0%	38.0%	39.0%	40.0%	36.0%	37.0%	37.5%	38.5%	39.5%	36.5%	37.5%	38.0%	39.0%	40.0%	33.9%	36.3%	37.4%
Coarse Agg. Vol. %	34.7%	32.9%	33.6%	31.9%	29.5%	34.7%	32.9%	33.6%	31.9%	29.5%	34.7%	32.9%	33.9%	32.1%	29.8%	34.5%	32.7%	33.6%	31.9%	29.5%	37.4%	33.1%	30.1%

4. Experimental Investigations

The bond strength of SCC was evaluated experimentally in three phases, as listed in Table 7. In PHASE I, pull-out testing was conducted on six SCC mixtures and six CVC mixtures to evaluate the bond strength of black (uncoated) deformed vertical reinforcing steel bars in tension according to RILEM/CEB/FIB [35]. For each concrete type, three mixtures containing crushed limestone aggregate with $\frac{3}{4}$, $\frac{1}{2}$, and $\frac{3}{8}$ in. (19, 13, and 10 mm) NMSA, and three mixtures containing gravel aggregate with $\frac{3}{4}$, $\frac{1}{2}$, and $\frac{3}{8}$ in. (19, 13, and 10 mm) NMSA were tested. All mixtures had the same SCM (25% Class F fly ash) and three specimens were tested from each mixture (total number of specimens was 36). In each specimen, #6 (19M) Grade 60 deformed bar was located vertically (such as in columns) at the center of an 8 in. (200 mm) cube and concrete was placed in the wooden form shown in Figure 4. A rigid plastic sheathing was attached to the top 4.25 in. (108 mm) of the bar, resulting in a bonded length of 3.75 in. (95 mm) (five times bar diameter). The forms were stripped after 24 h and the specimens were then moist-cured until day 28.

Table 7. Summary of the testing phases.

Testing Phase	Bar Orientation	Bar Size	No. of Tested Bars	Purpose
PHASE I	Vertical	#6 (19M)	36	Compare SCC vs. CVC
PHASE II	Horizontal	#6 (19M)	54	Evaluate top bar and SCC flowability effects
PHASE III	Vertical and Horizontal	#5 (16M) #8 (25M)	144	Evaluate bar location, orientation, coating, and size effects



Figure 4. Pull-out cube specimens' formwork (PHASE I).

A pull-out force was applied at a rate of 0.05 in./min. (1.3 mm/min) and the slip at the other end of the bar was measured using two linear variable differential transformers (LVDTs), as shown in Figure 5. The average compressive strength of the specimen ranged from 4.0 to 8.7 ksi (28 to 60 MPa) at the time of testing. The bond strength of each specimen was calculated at different slippage values: first, the critical bond strength corresponding to slippage of 0.01 in. (0.25 mm); and second, the ultimate bond strength at the maximum load, which is convenient for comparison purposes.

According to CEB-fib [36], the bar direction has a significant effect on the bond strength as horizontal bars have a larger area under which bleed water could accumulate in addition to the surface settlement due to lack of static stability. These effects can significantly lower the bond strength of horizontal bars compared to that of vertical ones. To evaluate the bond strength of horizontal bars (such as in beams) as well as the top-bar effect, in PHASE II, six 48 in. \times 48 in. \times 8 in. (1.2 m \times 1.2 m \times 0.2 m) wall specimens, shown in Figure 6, were cast: two walls using high-slump-flow SCC, two using low-slump-flow SCC, and two

using CVC. Each wall specimen had 9 #6 (M19) bars located horizontally in three rows, bottom (B), center (C), and top (T), as shown in Figure 7. The specimens were cast from the top with the flow of concrete perpendicular to the bar direction. Figure 8 shows the test setup using chuck's barrel and wedges of 0.7 in. (17.8 mm) diameter prestressing strand to restrain the movement of the hydraulic jack. Using the same procedures used for the pull-out of vertical bars, a total of 54 #6 (19M) Grade 60 black deformed horizontal steel bars were pulled out. These specimens were made using ready-mixed concrete and had an average concrete strength ranging from 7.1 to 8.3 ksi (49 to 57 MPa) at the time of testing. The test results indicated the effect of bar location and concrete type on the bond strength of horizontal bars.

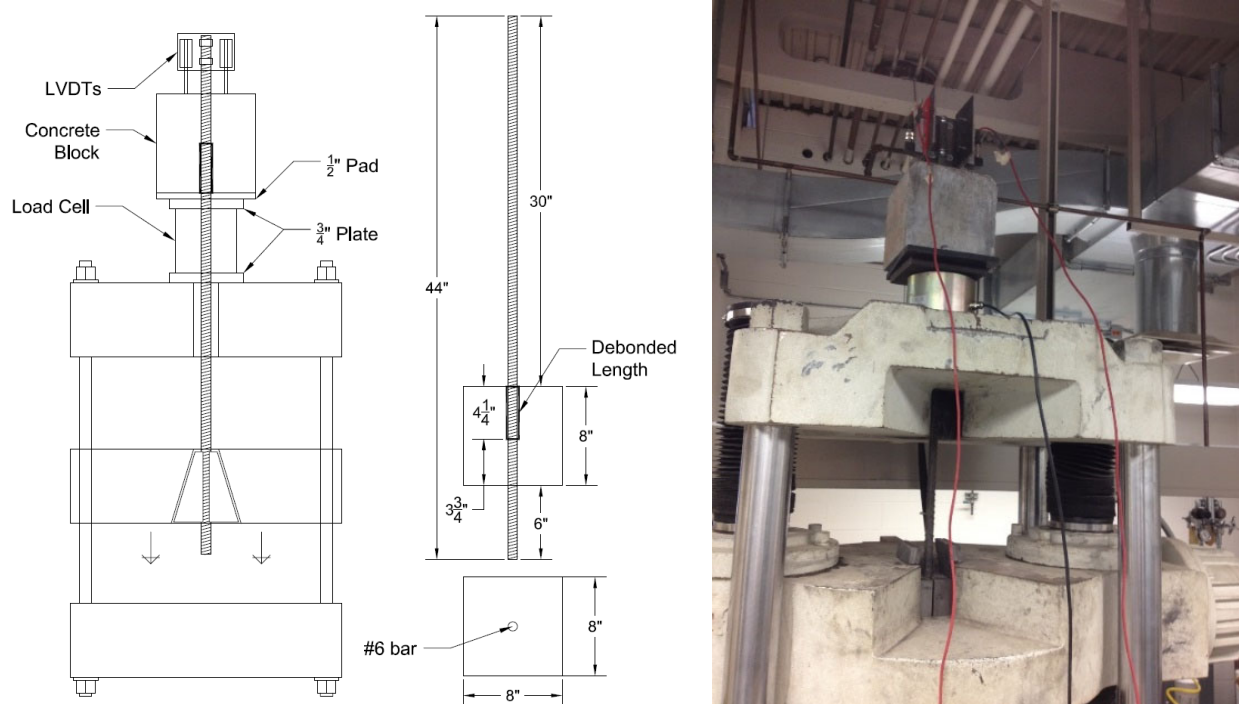


Figure 5. Pull-out test setup and specimen dimensions (PHASE I) (1 in. = 25.4 mm).



Figure 6. Pull-out wall specimen formwork (PHASE II).

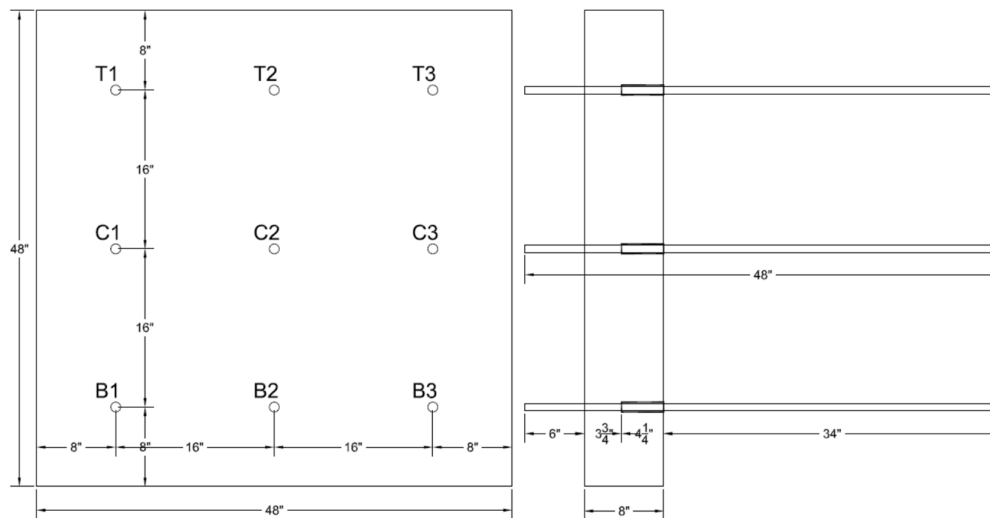


Figure 7. Pull-out wall specimen dimensions and bar arrangement (PHASE II) (1 in. = 25.4 mm).



Figure 8. Pull-out wall specimen test setup (PHASE II).

To provide a more comprehensive evaluation of the bond strength of horizontal and vertical bars, in PHASE III, twelve 48 in. \times 48 in. \times 8 in. (1.2 m \times 1.2 m \times 0.2 m) wall specimens and two 96 in. \times 48 in. \times 8 in. (2.4 m \times 1.2 m \times 0.2 m) slab were cast. A set of six walls and one slab were cast using high-slump-flow SCC and a similar set using CVC. The bars used in each set are #8 (25M) black (B), #8 (25M) epoxy-coated (C), and #5 (16M) black (b). Each wall specimen had nine bars located horizontally in three rows as shown in Figure 7 and was cast perpendicularly at the bar orientation. Two walls with typical embedded bars were cast for each bar size and type. One slab for each concrete type had 18 different bars located vertically in six rows with the arrangement shown in Figure 9 and was cast in parallel to the bar orientation. Figure 10 shows the test setup for #8 bars. This figure shows the use of a mechanical bar splice to restrain the movement of the hydraulic jack. Using the same procedures used for the former test, a total of 144 Grade 60 steel bars were pulled out as listed in Table 8. These specimens were made using ready-mixed concrete and had an average concrete strength of 4.4 to 7.4 ksi (30 to 51 MPa) for CVC and SCC, respectively, at the time of testing and slump of 2 in. (50 mm) for CVC and 26.25 in. (667 mm) for SCC. The testing results were used to evaluate the effect of bar location, concrete type, and bar orientation on the bond strength.

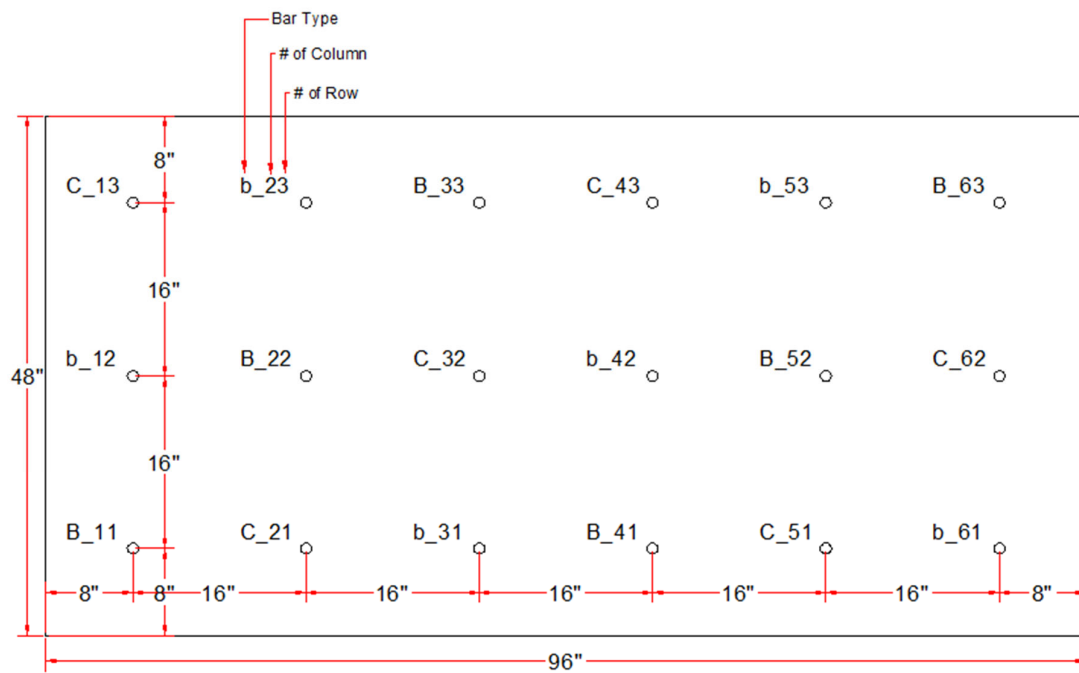


Figure 9. Pull-out slab specimen dimensions and bar arrangement (PHASE III) (1 in. = 25.4 mm).

Table 8. Test matrix showing the number of bond strength tests for each category (PHASE III).

ID	No. of Specimens	Concrete Type		Bar Orientation		Bar Size and Coating		
		CVC	SCC	Vertical	Horizontal	#5 Black	#8 Black	#8 Epoxy-Coated
S1	1	18		18		6	6	6
W1	2	18			18		18	
W2	2	18			18			18
W3	2	18			18	18		

Table 8. Cont.

ID	No. of Specimens	Concrete Type		Bar Orientation		Bar Size and Coating		
		CVC	SCC	Vertical	Horizontal	#5 Black	#8 Black	#8 Epoxy-Coated
S2	1		18	18		6	6	6
W4	2		18		18		18	
W5	2		18		18			18
W6	2		18		18	18		
TOTAL		72	72	36	108	48	48	48

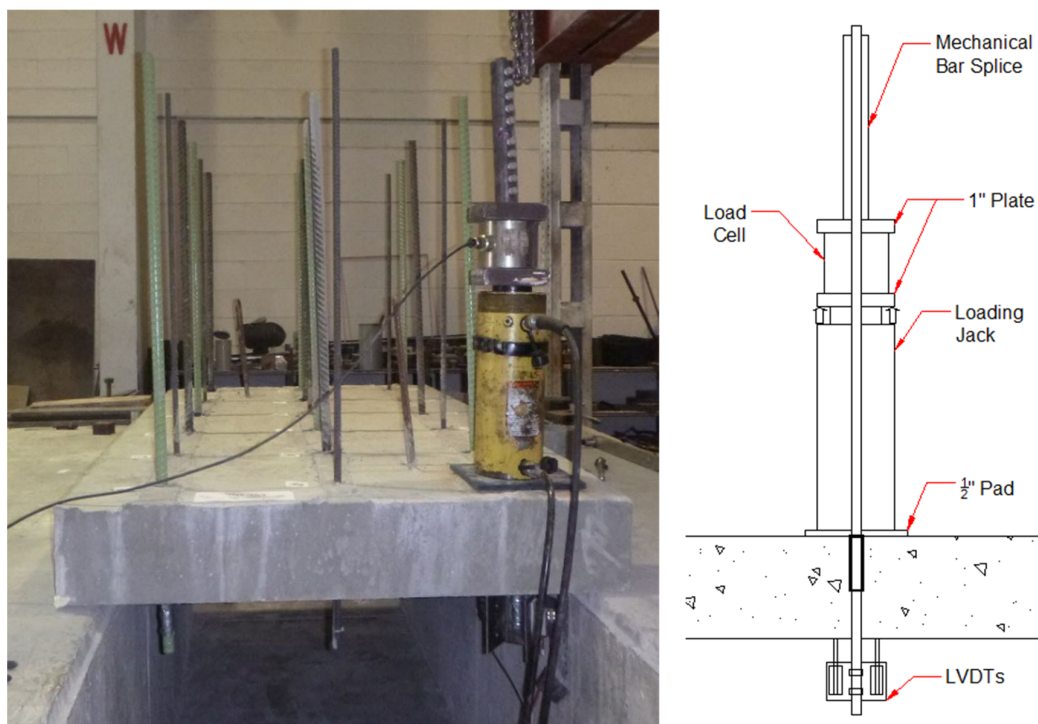


Figure 10. Pull-out slab specimen test setup (PHASE III).

5. Bond Test Results

The bond strength is obtained by dividing the load by the surface area of the embedded bar's length. The bond strength is calculated for two loading stages: load corresponding to 0.01 in. (0.25 mm) slippage; and maximum load. The results of bond strength of these two loading stages are summarized in tables in the appendix section for the three testing phases. The following subsections discuss these results and explain the effect of concrete type, bar location, size, orientation, and coating on the bond strength.

5.1. Bond Strength of SCC and CVC

The results of the PHASE I pull-out tests were used to compare the ultimate bond strength of SCC and CVC. Figure 11 shows the pull-out bond strength of 36 vertical deformed #6 reinforcing bars in tension versus $\sqrt{f'_c}$ for SCC and CVC mixtures. The two linear relationships indicate that the pull-out bond strength of SCC was consistently lower than that of CVC, which agrees with earlier studies [6,7,9]. Therefore, a bond strength modification factor of 1.3 is proposed for vertical bars when used with SCC mixtures. Pull-out test results shown in Appendix A also indicate that mixtures containing limestone aggregate exhibited slightly higher bond strength than those containing gravel aggregate.

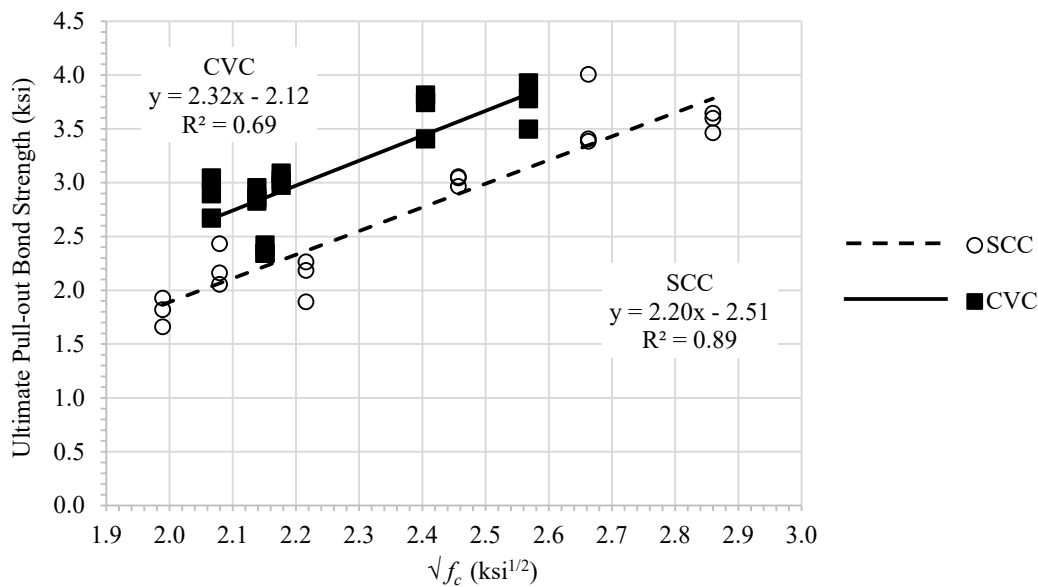


Figure 11. Pull-out bond strength versus $\sqrt{f_c}$ of SCC and CVC mixtures (1 ksi = 6.9 MPa).

5.2. Top-Bar Effect

The results of PHASE II pull-out tests were used to evaluate the top-bar effect in SCC and CVC mixtures. These results are shown in Appendix A. Figure 12 shows the normalized bond strength by dividing it by $\sqrt{f_c}$ to compare the change in bond strength of 54 horizontal deformed reinforcing bars with height. This figure indicates that there was no significant difference in the bond strength of horizontal bars between low-slump-flow SCC and CVC mixtures, but there was a slight difference between low-slump-flow SCC and high-slump-flow SCC. The one-way analysis of variance (ANOVA) of pull-out test data for the three groups of mixtures confirmed this conclusion at a 95% confidence level ($p = 0.38$). The figure also shows a reduction in the bond strength as the distance from the bottom of the form increases (top-bar effect). This effect was more evident in CVC and low-slump-flow SCC mixtures than it was in high-slump-flow SCC mixtures, indicating that the top-bar effect was dependent on the rheological properties of SCC.

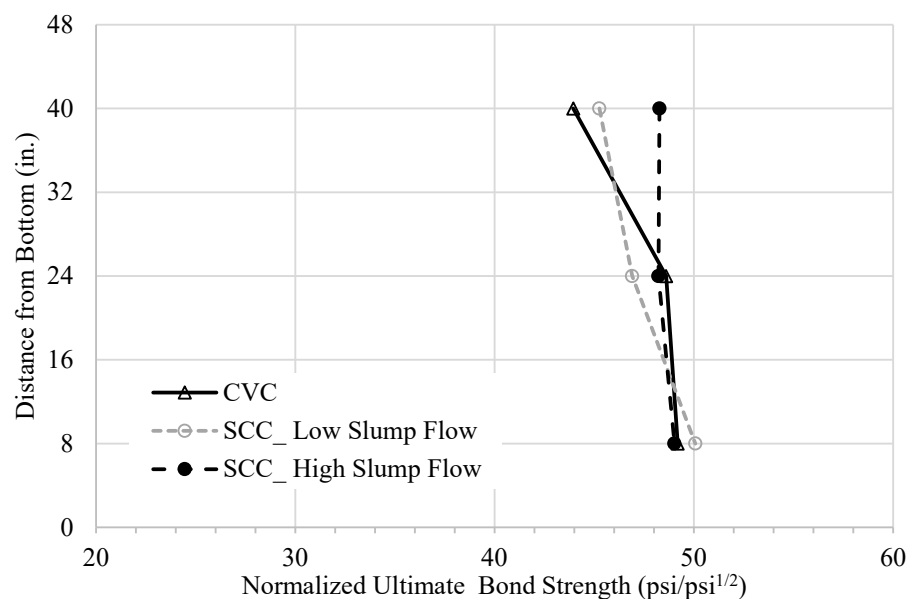
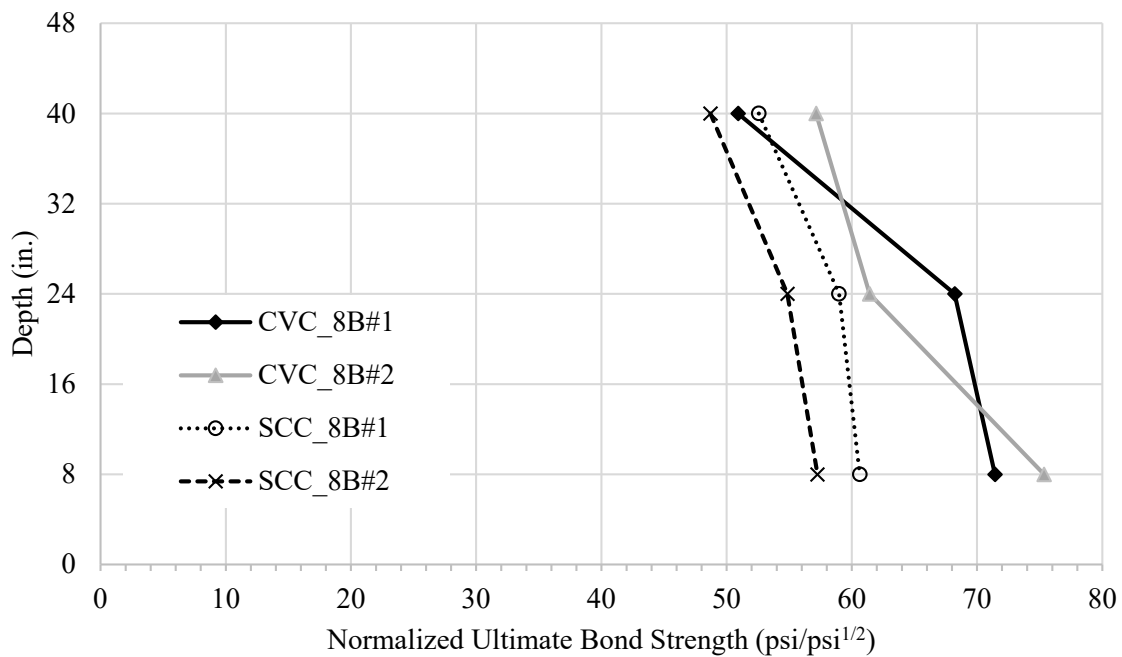
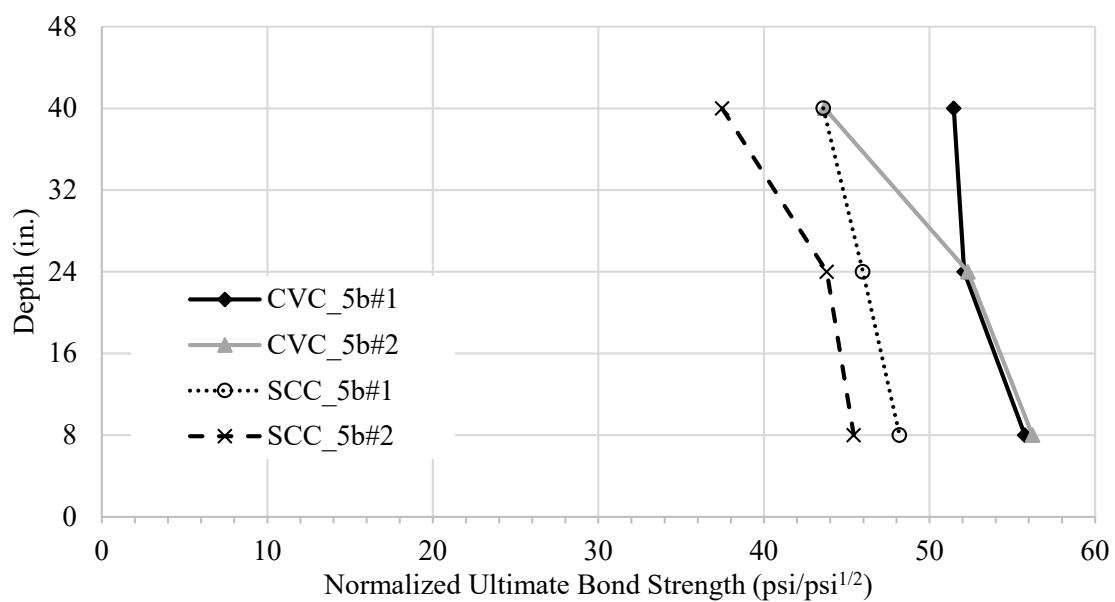


Figure 12. Top-bar effect on bond strength of # 6 (19M) black horizontal bars in CVC and SCC mixtures with low and high slump flow (1 in. = 25.4 mm).

Due to the high scatter of the previous results, additional pull-out tests were conducted in PHASE III to confirm the top-bar effect on the bond strength in CVC and SCC. Figure 13 shows the variation in bond strength with the height of different bar configurations in CVC and SCC. Each point represents the average of the results of three bars. These figures show that the upper bars have less bond strength than the bottom ones for both CVC and SCC. To provide a rational evaluation of the effect of concrete type on the top-bar effect, a statistical analysis was conducted and indicated that there is no statistically significant difference between CVC and SCC with respect to top-bar effect. Therefore, the development length modification factor of 1.3 for top horizontal bars with more than 12 in. (300 mm) of fresh concrete cast below them could conservatively be applied to SCC regardless of the slump flow.



(a)



(b)

Figure 13. Cont.

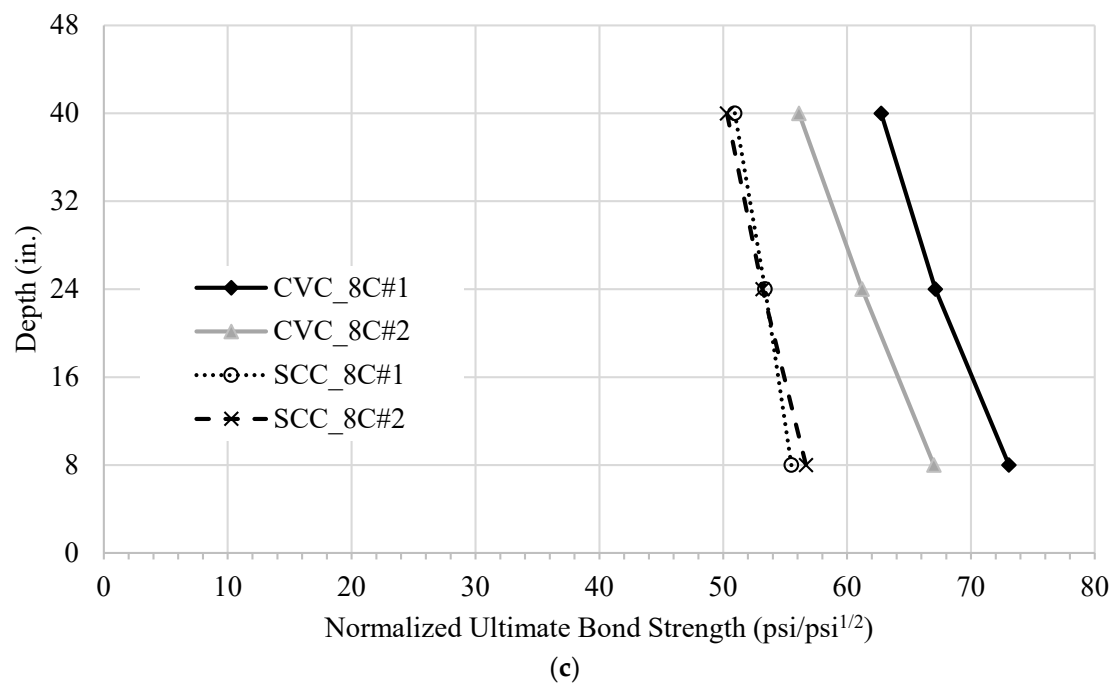


Figure 13. Variation in ultimate bond strength due to top-bar effect (1 in. = 25.4 mm). (a) #8 (25M) black bars; (b) #5 (16M) black bars; (c) #8 (25M) epoxy-coated bars.

5.3. Bond of Horizontal Bars

Figures 14 and 15 present comparisons between the bond strength of horizontal bars in CVC and SCC at 0.01 in. (0.25 mm) slippage (critical load) and ultimate load, respectively. At the critical loading stage, #8 (25M) and #5 (16M) black bars show similar bond strength in CVC and SCC. Only #8 (25M) epoxy-coated bars presented higher critical bond strength in SCC than CVC. At the ultimate loading stage, all bars show lower bond strength in SCC than CVC by approximately 17%. Figures 16 and 17 show the variance between the critical and ultimate bond strength of horizontal bars in CVC and SCC, respectively. They show that the bars in CVC develop significant bond strength after 0.01 in. (0.25 mm) slippage, especially for #8 (25M) bars, which is dissimilar to those in SCC. This explains the lower ultimate bond strength of SCC at the ultimate loading stage after being similar to CVC or lower at the critical loading stage.

5.4. Bond of Vertical Bars

Figures 18 and 19 present comparisons between the bond strength of vertical bars in CVC and SCC at 0.01 in. (0.25 mm) slippage and ultimate load, respectively. At the critical loading stage, #8 (25M) black bars show similar bond strength in CVC and SCC. However, #5 (16M) black and #8 (25M) epoxy-coated bars presented lower and higher, respectively, critical bond strength in SCC than in CVC. At the ultimate loading stage, #5 (16M) black bars show lower bond strength in SCC than CVC by 11%. ANOVA confirmed that no significant difference at a 95% confidence level existed between the ultimate bond strength of the #8 (25M) black and epoxy-coated vertical bars in CVC ($p = 0.06$) and SCC ($p = 0.91$). Figures 20 and 21 show the critical and ultimate bond strength of vertical bars in CVC and SCC, respectively. They show that vertical epoxy-coated bars in CVC and SCC develop significant bond strength after 0.01 in. (0.25 mm) slippage. This explains the lower ultimate bond strength of SCC after being similar to CVC or lower at critical stage. ANOVA confirmed that there is no significant difference between the critical and the ultimate bond strength of #5 (16M) black bars in SCC mixtures ($p = 0.13$).

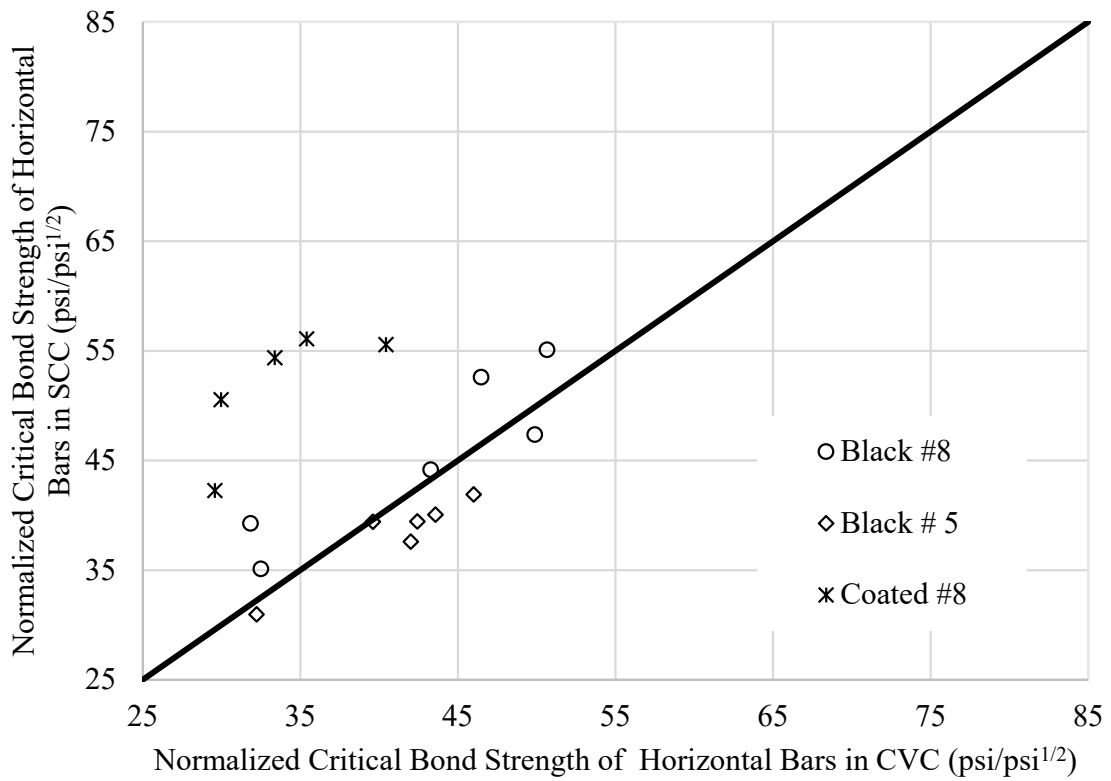


Figure 14. Relationship between critical bond strength of horizontal bars in CVC and SCC.

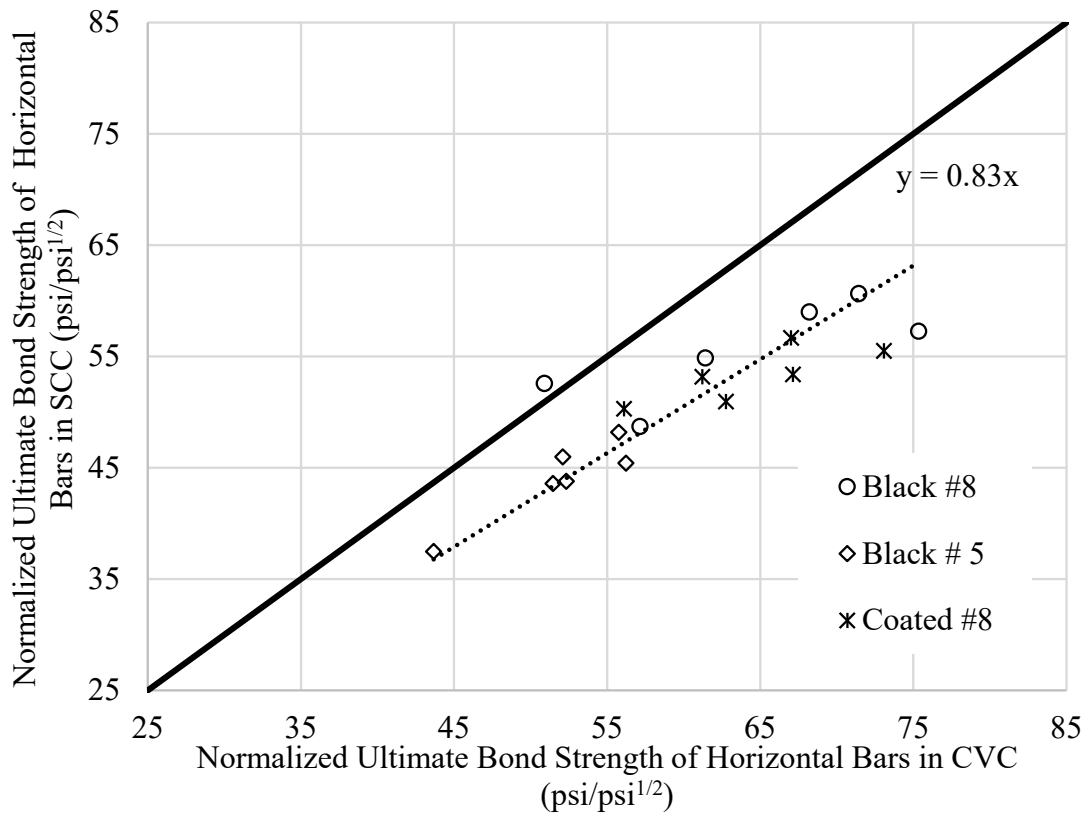


Figure 15. Relationship between ultimate bond strength of horizontal bars in CVC and SCC.

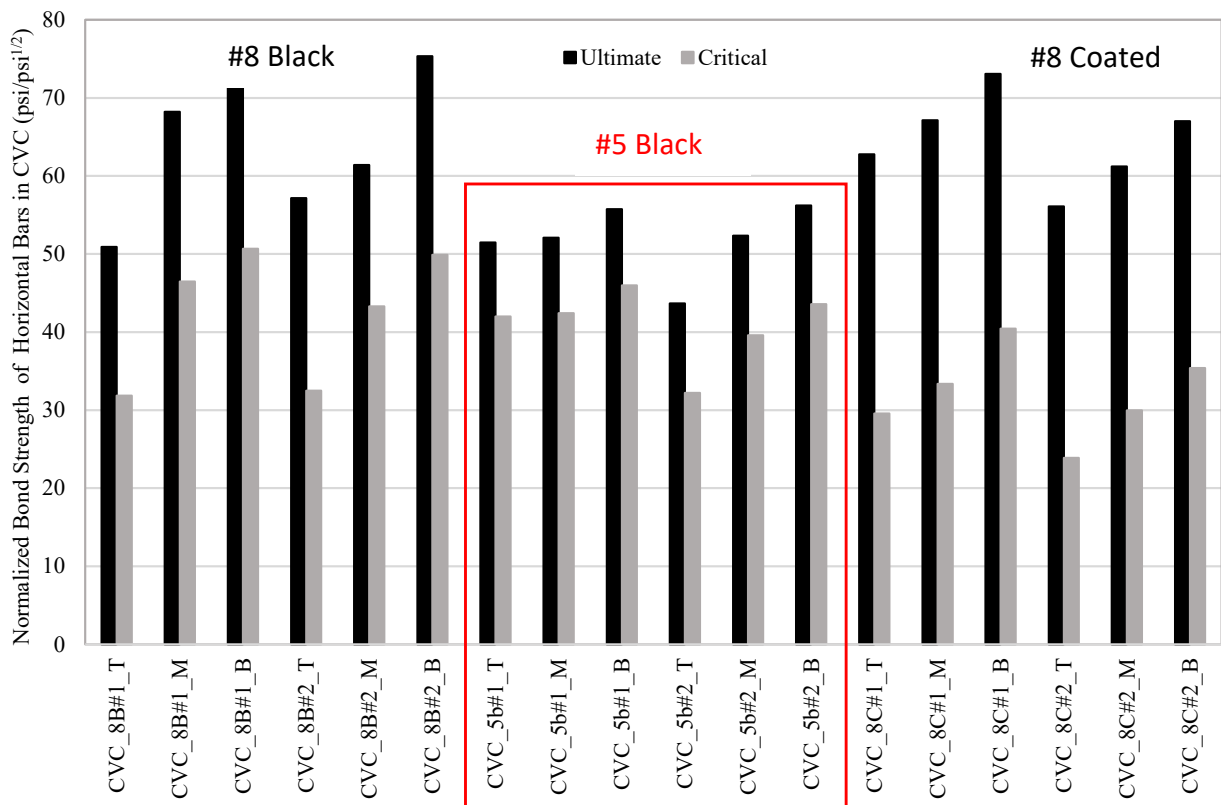


Figure 16. Normalized critical and ultimate loading stages of horizontal bars in CVC walls.

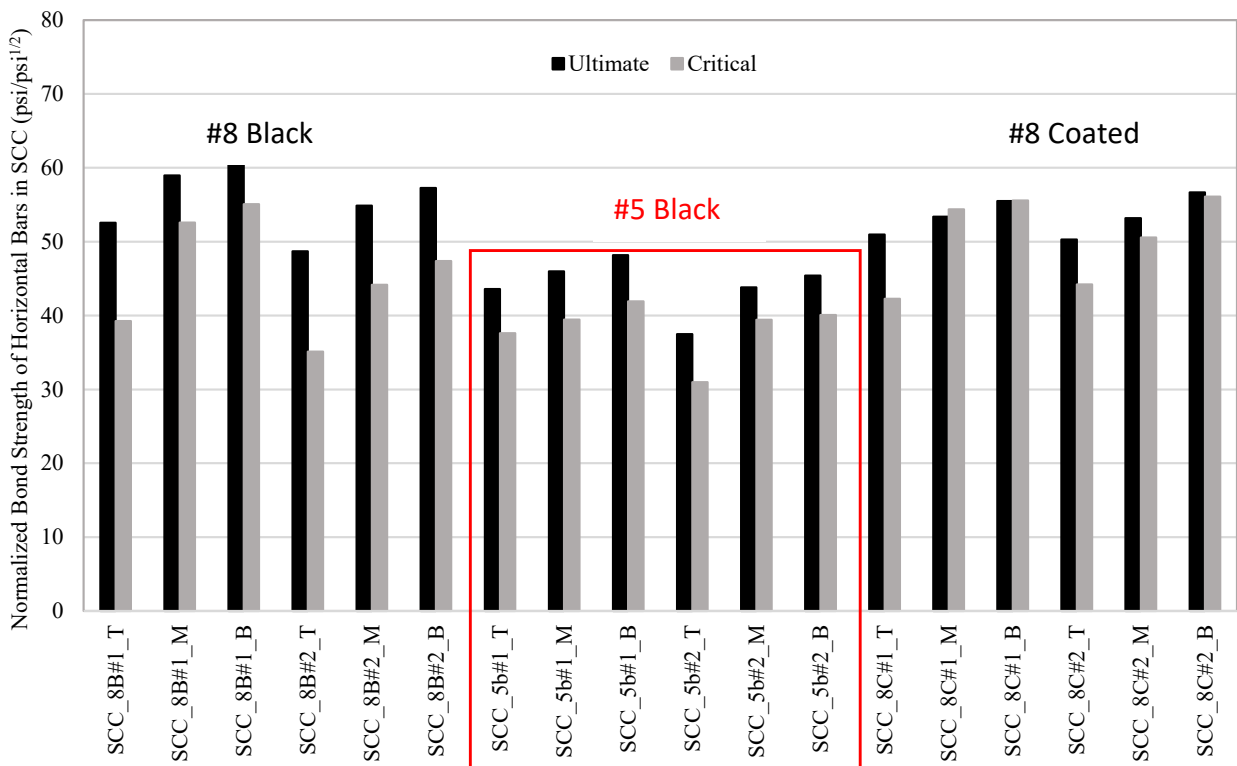


Figure 17. Normalized critical and ultimate loading stages of horizontal bars in SCC walls.

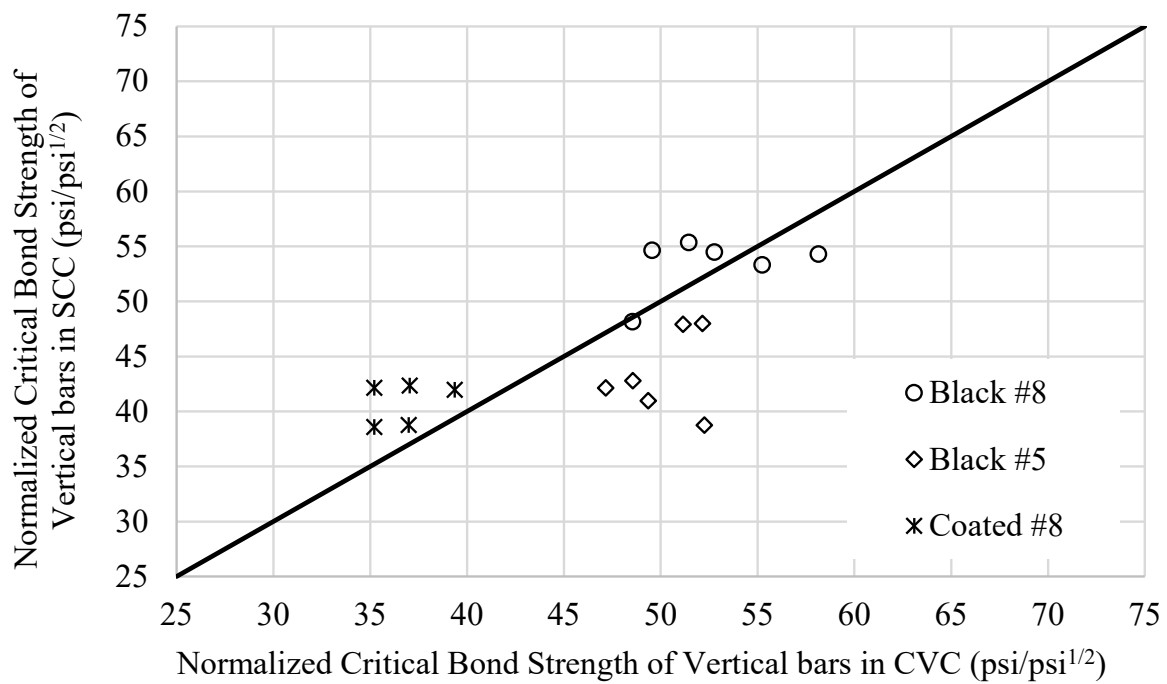


Figure 18. Relationship between critical bond strength of vertical bars in CVC and SCC.

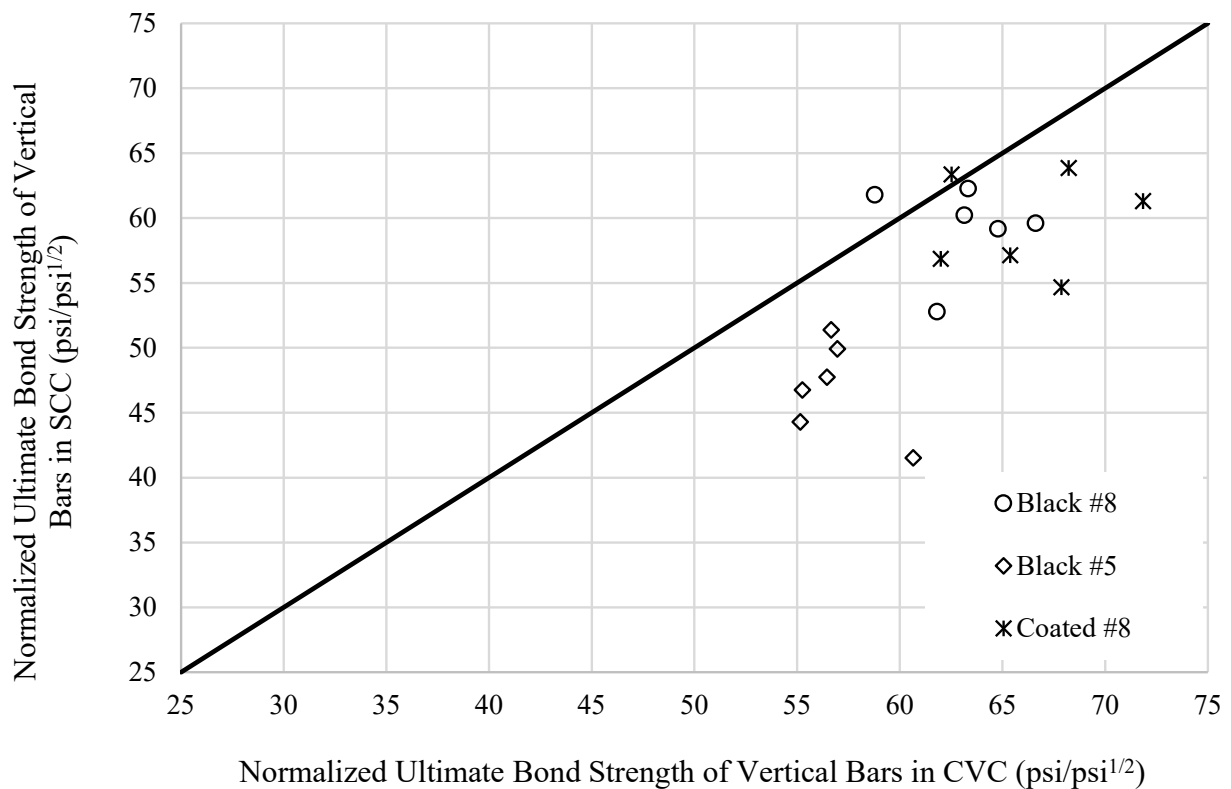


Figure 19. Relationship between ultimate bond strength of vertical bars in CVC and SCC.

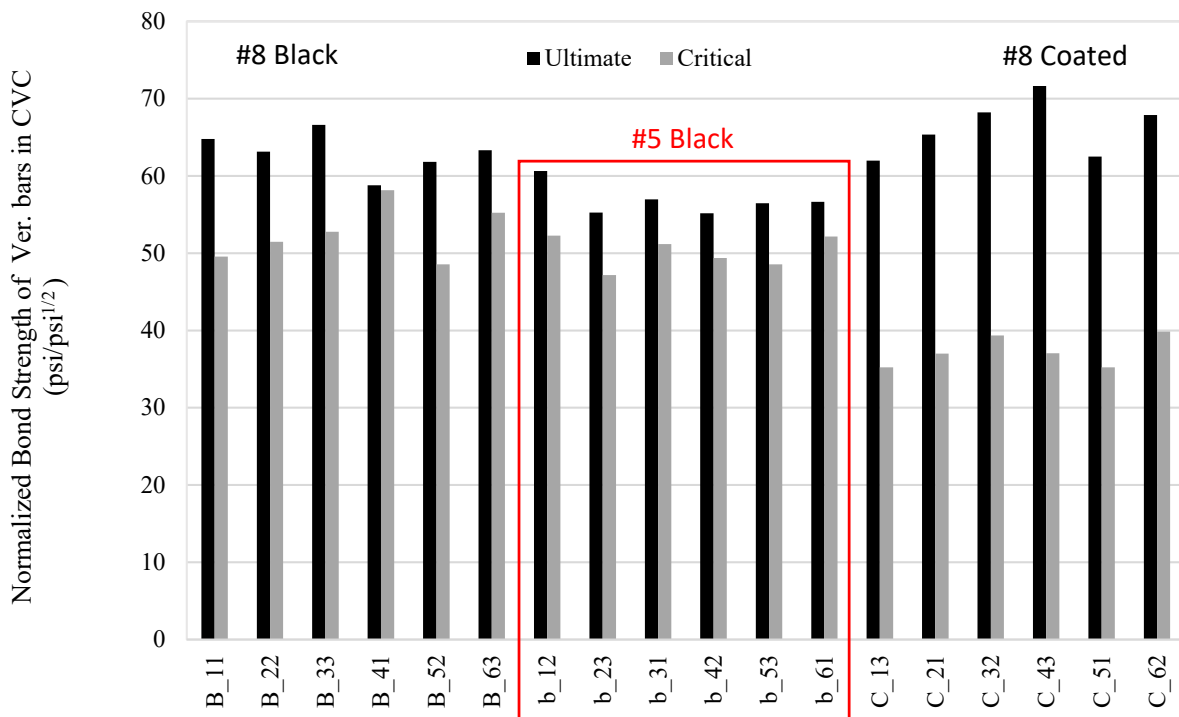


Figure 20. Normalized critical and ultimate bond strength of vertical bars in CVC slabs.

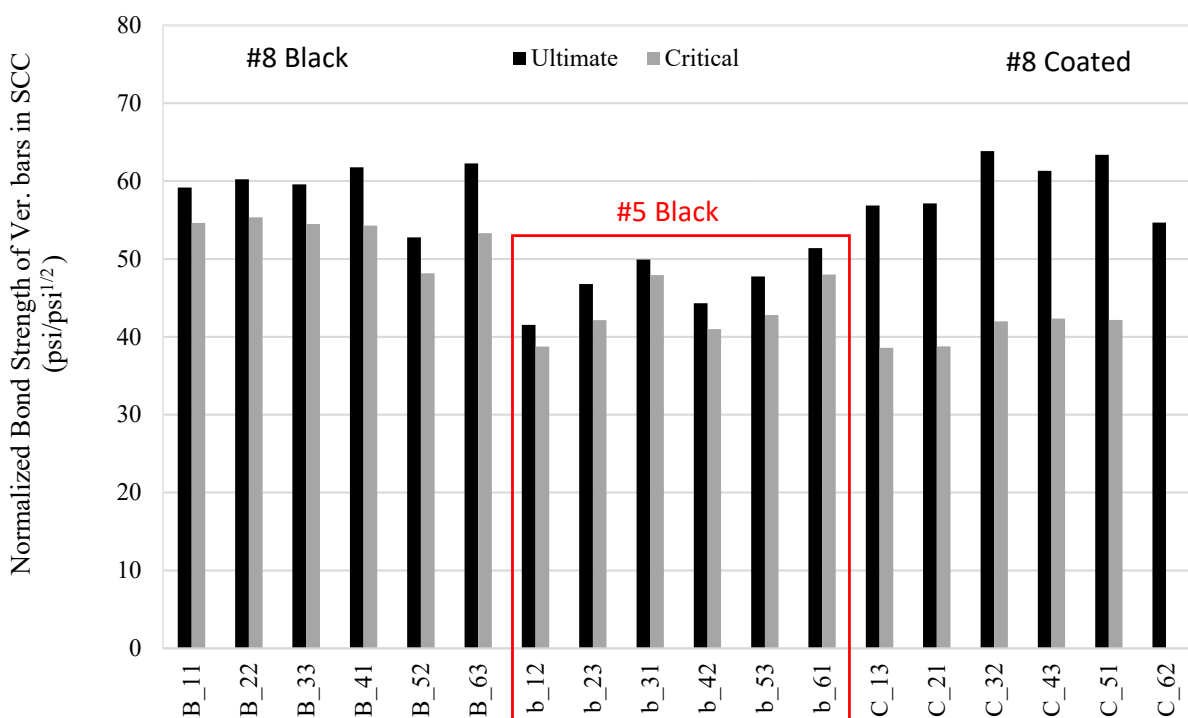


Figure 21. Normalized critical and ultimate bond strength of vertical bars in SCC slabs.

5.5. Effect of Bar Orientation

Figures 22 and 23 show the comparison between the bond strength of the vertical and horizontal bars at the critical and ultimate loading stages in CVC and SCC, respectively. The horizontal bars represent those located at the bottom 8 in. (200 mm) of the wall's height. These figures show that 91% and 83% of the CVC and SCC data points, respec-

tively, are $\pm 20\%$ away from the line of equality. This indicates that bar orientation has a slightly more pronounced effect on the bond strength in SCC than in CVC. ANOVA was performed to evaluate the significance of the difference between the two orientations at a 95% confidence level. The analysis results indicated that there is a significant difference between the bond strength of vertical and horizontal black bars in CVC mixtures, while in SCC mixtures, the significant difference is between the bond strength of vertical and horizontal epoxy-coated bars.

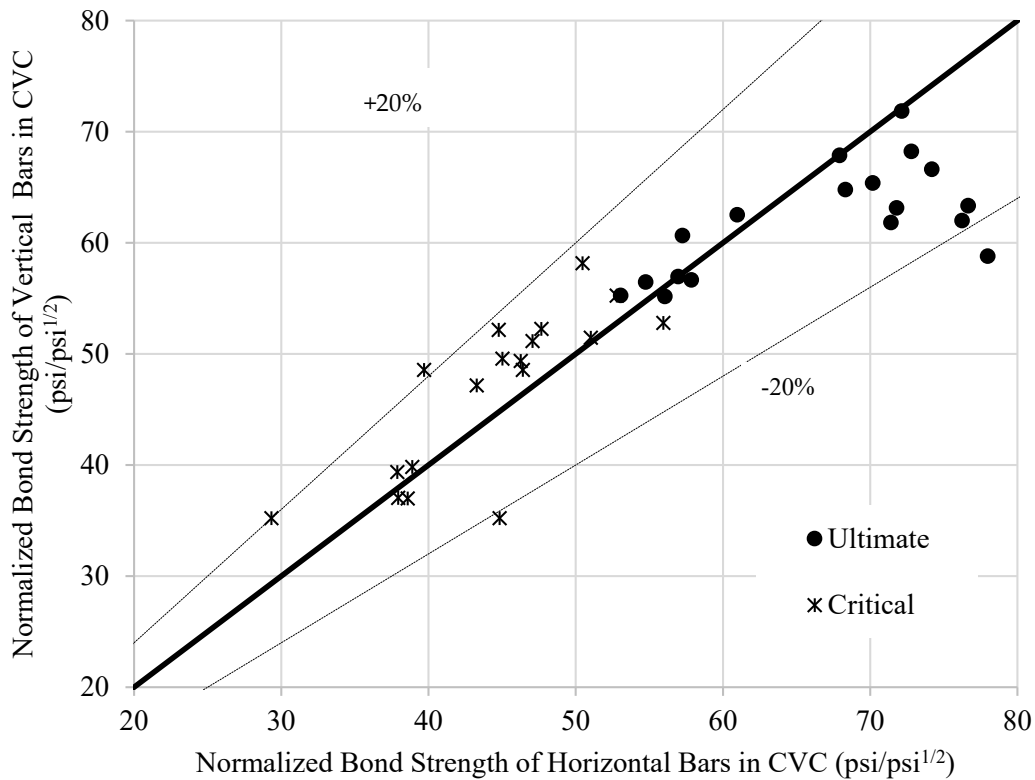


Figure 22. Relationship between the bond strength of the horizontal and vertical bars in CVC.

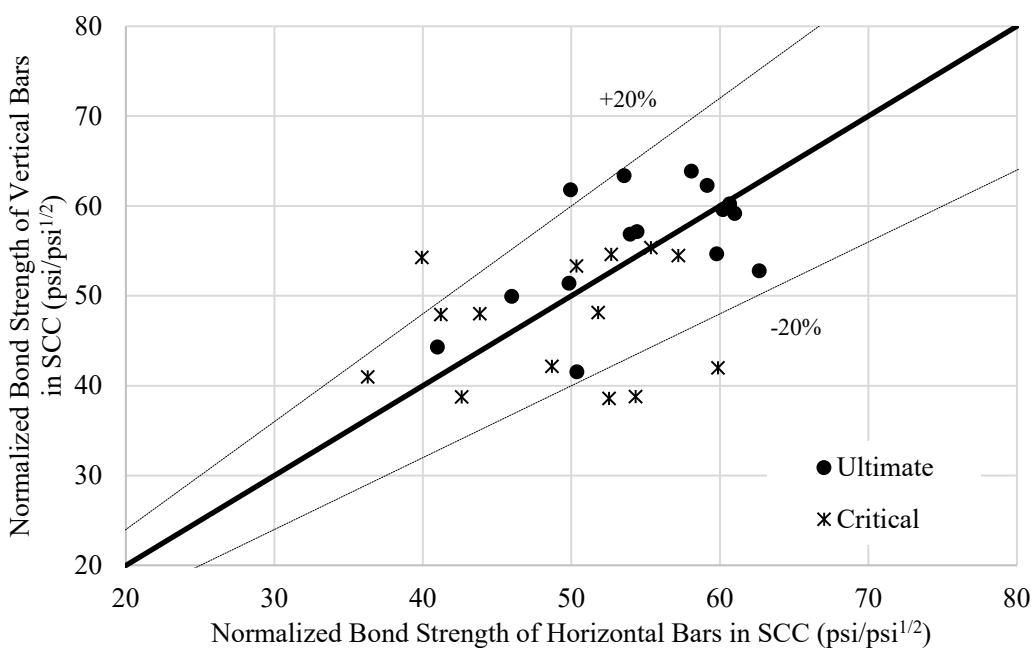


Figure 23. Relationship between the bond strength of the horizontal and vertical bars in SCC.

5.6. Bond Strength Prediction

The design provisions in ACI 318 [1] for the development and splice length of straight reinforcement in tension are based on the expressions developed by Orangun, Jirsa, and Breen in the ACI 408R report [37]. This model predicts the bond strength of bars without confining transverse reinforcement by testing beams under flexure. This model expresses the average bond strength at failure (u_c) and is represented by the following expression:

$$\frac{u_c}{\sqrt{f'_c}} = 1.22 + 3.23 \frac{c_{min}}{d_b} + 53 \frac{d_b}{l_d}$$

where c_{min} = smaller value of the minimum concrete cover or half of the clear spacing between bars; l_d = development or splice length; d_b = bar diameter; and f'_c = concrete compressive strength.

This expression was used to evaluate the critical bond strength from the test results of this study. Figures 24–27 show the measured and predicted values of the normalized bond strength for different bar configurations. These figures indicate that this expression overestimates the bond strength of all tested bars, except #8 (25M) black bars in both CVC and SCC mixtures (Figure 25) and #8 (25M) epoxy-coated horizontal bars in SCC (Figure 27).

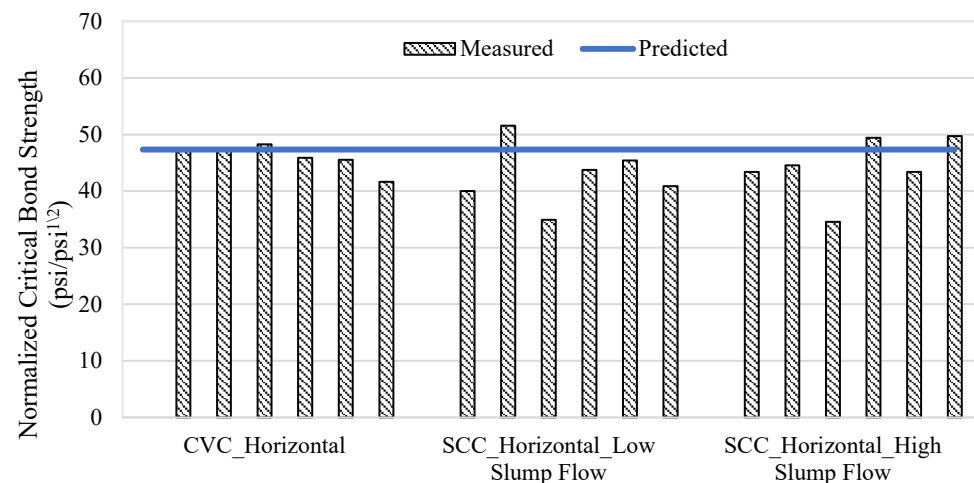


Figure 24. Relationship between measured and predicted bond strength of #6 (19M) black horizontal bars.

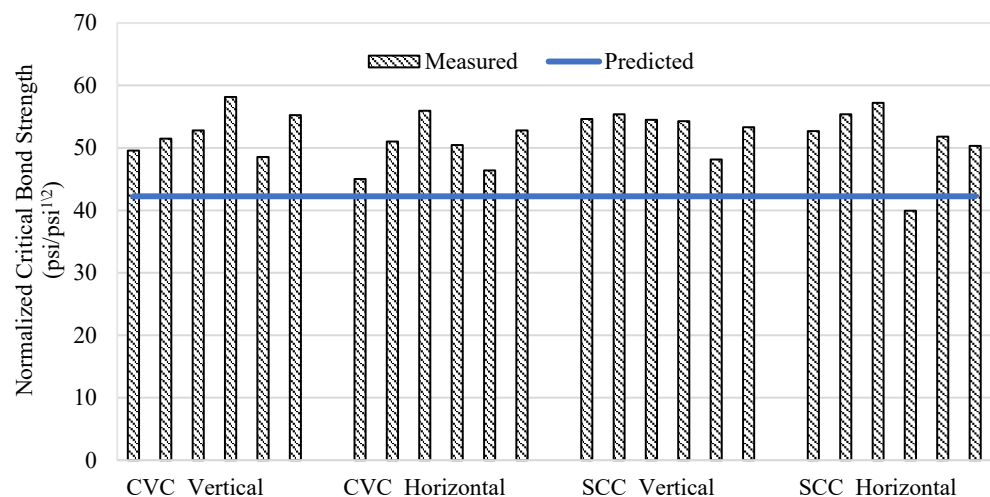


Figure 25. Relationship between measured and predicted bond strength of #8 (25M) black bars.

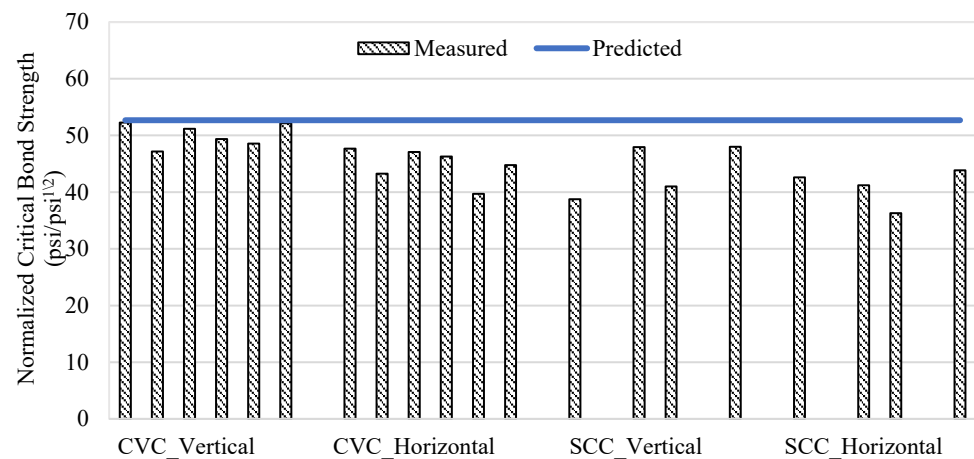


Figure 26. Relationship between measured and predicted bond strength of #5 (16M) black bars.

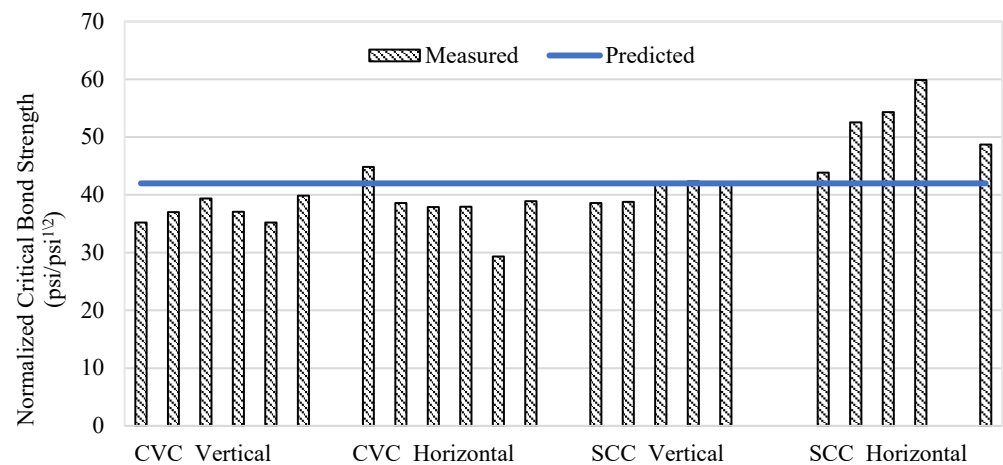


Figure 27. Relationship between measured and predicted bond strength of #8 (25M) epoxy-coated bars.

6. Conclusions

Based on the results of the experimental investigation presented in this study, the following conclusions can be drawn:

1. The pull-out bond strength of horizontal reinforcing steel bars cast in high-slump-flow SCC was similar to that of bars cast in CVC, but the pull-out bond strength of horizontal reinforcing steel bars cast in medium- and low-slump-flow SCC was lower than that of bars cast in CVC.
2. A development length modification factor of 1.3 was recommended to account for the difference between the bond strength of SCC and CVC.
3. The top-bar effect was lower in high-slump-flow SCC than that in low-slump-flow SCC and CVC. Therefore, the development length modification factor of 1.3 (ACI 318-19) for top horizontal bars with more than 12 in. (300 mm) of fresh concrete cast below them could conservatively be applied to SCC regardless of the slump flow.
4. The orientation of the bar could have a significant effect on the bond strength, in both CVC and SCC, depending on bar's size and coating.
5. The bond strength prediction using ACI 408R-03 overestimates the bond strength of # 6 (19M) black bars in SCC, #8 (25M) epoxy-coated in CVC and #5 (16M) black bars in both concrete types.

Author Contributions: Conceptualization, G.M.; Methodology, M.A.; Formal analysis, M.A. and G.M.; Writing—original draft, M.A.; Writing—review & editing, G.M. All authors have read and agreed to the published version of the manuscript.

Funding: This research was partially funded by the National Cooperative Highway Research Program grant number NCHRP 18-16.

Data Availability Statement: Data are contained within the article.

Conflicts of Interest: The authors declare no conflict of interest.

Appendix A

Table A1. Pull-out test results of #6 (19M) vertical bars in 8 in. (200 mm) cube specimens (PHASE I). (1 in. = 25.4 mm).

Coarse Aggregate		Mixture Type	f_c' (psi)	Parameter	Specimen			Average	COV	
Type	NMSA				#1	#2	#3			
Gravel	3/4"	SCC 2111	4323	Ultimate Load (lb)	21,500	19,100	18,160	19,587	8.8%	
				Bond Strength (psi)	2433	2162	2055	2217	8.8%	
				Load at Slip 0.01 in. (lb)	14,780	16,730	17,174	16,228	7.8%	
				Failure Mode	Slippage	Slippage	Slippage	N/A	N/A	
		CVC No. 67	4571	Ultimate Load (lb)	25,000	25,300	26,100	25,467	2.2%	
				Bond Strength (psi)	2829	2863	2954	2882	2.2%	
				Load at Slip 0.01 in. (lb)	23,190	22,800	23,976	23,322	2.6%	
				Failure Mode	Slippage	Slippage	Slippage	N/A	N/A	
		1/2"	SCC 2221	3956	Ultimate Load (lb)	17,020	14,670	16,080	15,923	7.4%
					Bond Strength (psi)	1926	1660	1820	1802	7.4%
					Load at Slip 0.01 in. (lb)	15,095	14,042	13,633	14,257	5.3%
			CVC No. 78	4626	Failure Mode	Slippage	Slippage	Slippage	N/A	N/A
	Ultimate Load (lb)				21,400	20,700	20,700	20,933	1.9%	
	Bond Strength (psi)				2422	2343	2343	2369	1.9%	
	3/8"	SCC 2222	4911	Load at Slip 0.01 in. (lb)	15,631	16,846	18,365	16,947	8.1%	
				Failure Mode	Slippage	Slippage	Slippage	N/A	N/A	
				Ultimate Load (lb)	20,000	19,300	16,730	18,677	9.2%	
				Bond Strength (psi)	2264	2184	1893	2114	9.2%	
				Load at Slip 0.01 in. (lb)	18,444	17,555	16,730	17,576	4.9%	
				Failure Mode	Slippage	Slippage	Splitting	N/A	N/A	
		CVC No. 8	4738	Ultimate Load (lb)	26,700	27,300	26,300	26,767	1.9%	
				Bond Strength (psi)	3022	3090	2977	3029	1.9%	
				Load at Slip 0.01 in. (lb)	24,850	25,350	23,630	24,610	3.6%	
				Failure Mode	Slippage	Splitting	Slippage	N/A	N/A	
Ultimate Load (lb)				29,900	30,100	35,400	31,800	9.8%		
Bond Strength (psi)				3384	3407	4006	3599	9.8%		
Limestone	3/4"	SCC 2111	7090	Load at Slip 0.01 in. (lb)	28,955	27,450	30,370	28,925	5.0%	
				Failure Mode	Slippage	Slippage	Slippage	N/A	N/A	
				Ultimate Load (lb)	23,600	25,600	26,900	25,367	6.6%	
				Bond Strength (psi)	2671	2897	3044	2871	6.6%	
	CVC No. 67	4269	Load at Slip 0.01 in. (lb)	22,241	21,388	16,766	20,132	14.6%		
			Failure Mode	Slippage	Slippage	Splitting	N/A	N/A		

Table A1. Cont.

Coarse Aggregate		Mixture Type	f_c' (psi)	Parameter	Specimen			Average	COV
Type	NMSA				#1	#2	#3		
Limestone	1/2"	SCC 2221	8177	Ultimate Load (lb)	30,600	32,200	31,800	31,533	2.6%
				Bond Strength (psi)	3463	3644	3599	3569	2.6%
				Load at Slip 0.01 in. (lb)	N/A	28,640	29,500	29,070	2.1%
				Failure Mode	N/A	Slippage	Slippage	N/A	N/A
		CVC No. 78	5783	Ultimate Load (lb)	30,100	33,100	33,700	32,300	6.0%
				Bond Strength (psi)	3407	3746	3814	3656	6.0%
	Load at Slip 0.01 in. (lb)			25,930	30,300	29,520	28,583	8.2%	
			Failure Mode	Splitting	Splitting	Splitting	N/A	N/A	
	3/8"	SCC 2222	6037	Ultimate Load (lb)	26,900	26,200	27,000	26,700	1.6%
				Bond Strength (psi)	3044	2965	3056	3022	1.6%
				Load at Slip 0.01 in. (lb)	24,347	21,299	25,071	23,572	8.5%
				Failure Mode	Splitting	Slippage	Splitting	N/A	N/A
		CVC No. 8	6593	Ultimate Load (lb)	33,400	30,900	34,700	33,000	5.9%
				Bond Strength (psi)	3780	3497	3927	3735	5.9%
	Load at Slip 0.01 in. (lb)			32,900	28,100	34,000	31,667	9.9%	
		Failure Mode	Splitting	Splitting	Splitting	N/A	N/A		

Table A2. Pull-out test results of #6 (19M) horizontal bars in wall specimens (PHASE II).

Mixture Type	f_c' (ksi)	Load Stage	Bar Location	Wall Specimen #1			Wall Specimen #2			Average	COV
				Bar #1	Bar #2	Bar #3	Bar #1	Bar #2	Bar #3		
SCC (Low slump flow)	8.3	Load at 0.01 in. Slip (lb)	Top	36,570	32,851	28,321	37,475	29,656	30,276	32,525	11.7%
			Center	37,905	32,135	35,807	34,472	34,758	37,142	35,370	5.8%
			Bottom	32,217	41,528	28,130	35,235	36,570	32,898	34,430	13.2%
		Maximum Load (lb)	Top	41,385	35,854	34,186	40,002	32,898	34,376	36,450	9.5%
			Center	38,429	35,425	38,095	36,521	38,429	39,764	37,777	4.1%
			Bottom	41,766	41,814	38,191	38,810	37,285	44,103	40,328	6.5%
SCC (High slump flow)	7.1	Load at 0.01 in. Slip (lb)	Top	31,277	27,511	31,802	32,708	39,907	39,716	33,820	14.7%
			Center	32,231	31,659	31,945	39,478	38,858	35,807	34,996	10.2%
			Bottom	32,326	33,184	25,746	36,808	32,326	37,046	32,906	12.5%
		Maximum Load (lb)	Top	34,948	36,999	38,763	36,856	42,672	43,054	38,882	8.5%
			Center	36,236	34,948	35,592	40,861	43,101	42,291	38,838	9.4%
			Bottom	41,671	38,095	37,952	40,575	37,666	40,956	39,486	4.5%
CVC	7.6	Load at 0.01 in. Slip (lb)	Top	31,420	30,228	37,571	28,750	33,041	29,847	31,810	10.0%
			Center	32,469	39,144	35,711	37,523	32,708	37,666	35,870	7.7%
			Bottom	36,283	36,379	37,189	35,378	35,091	32,088	35,401	5.1%
		Maximum Load (lb)	Top	34,758	35,330	40,765	30,991	35,664	34,853	35,394	8.8%
			Center	35,044	44,532	38,906	39,907	34,281	42,196	39,144	10.2%
			Bottom	40,336	40,431	42,148	39,716	38,810	36,236	39,613	5.0%

Table A3. Pull-out test results of horizontal #8 (25M) and #5 (16M) bars in CVC walls (PHASE III).

Bar Type	Load Stage	Bar Location	Wall Specimen #1			Wall Specimen #2			Average (lb)	COV (%)
			Bar #1	Bar #2	Bar #3	Bar #1	Bar #2	Bar #3		
#8 Black	Load at 0.01 in. Slip (lb)	Top	23,422	23,329	23,145	21,320	26,057	24,339	23,602	6.6%
		Center	31,090	37,419	33,493	33,861	31,259	30,377	32,917	7.9%
		Bottom	32,938	37,327	40,930	37,112	34,139	38,830	36,879	8.0%
	Max. Load (lb)	Top	37,281	35,433	39,036	41,485	43,009	40,930	39,529	7.2%
		Center	45,966	50,585	53,172	47,767	42,732	44,303	47,421	8.3%
		Bottom	49,985	52,526	54,281	57,053	52,248	56,083	53,696	4.9%
#5 Black	Load at 0.01 in. Slip (lb)	Top	19,911	19,264	19,079	12,473	16,954	15,245	17,154	16.8%
		Center	20,327	NA	18,894	19,865	15,568	19,495	18,830	10.1%
		Bottom	22,036	20,003	21,759	21,389	18,340	20,696	20,704	6.6%
	Max. Load (lb)	Top	24,346	23,606	23,422	19,356	21,112	20,096	21,990	9.4%
		Center	25,870	22,036	24,346	25,362	22,128	25,085	24,138	6.9%
		Bottom	26,471	24,530	26,332	25,916	25,316	26,748	25,886	3.2%
#8 Epoxy Coated	Load at 0.01 in. Slip (lb)	Top	22,128	22,636	24,253	39,129	43,425	48,414	33,331	35.1%
		Center	24,068	27,025	26,794	48,737	44,903	49,246	36,796	32.6%
		Bottom	34,878	30,028	29,473	56,129	47,444	52,849	41,800	28.3%
	Max. Load (lb)	Top	47,490	48,229	50,770	N/A	19,541	20,558	37,318	42.4%
		Center	51,324	55,066	50,308	N/A	23,191	23,976	40,773	38.7%
		Bottom	59,317	54,604	56,637	29,520	N/A	30,259	46,067	32.3%

Table A4. Pull-out test results of horizontal #8 (25M) and #5 (16M) bars in SCC walls (PHASE III).

Bar Type	Load Stage	Bar Location	Wall Specimen #1			Wall Specimen #2			Average (lb)	COV (%)
			Bar #1	Bar #2	Bar #3	Bar #1	Bar #2	Bar #3		
#8 Black	Load at 0.01 in. Slip (lb)	Top	37,281	35,433	39,036	35,533	31,167	33,768	35,370	7.7%
		Center	45,966	50,585	53,172	42,732	37,855	45,751	46,010	11.9%
		Bottom	49,985	52,526	54,281	38,087	49,421	48,027	48,721	11.6%
	Max. Load (lb)	Top	51,786	48,276	49,569	44,210	44,025	50,401	48,045	6.8%
		Center	56,037	54,004	57,838	52,849	48,691	54,604	54,004	5.8%
		Bottom	57,884	57,561	57,145	47,398	59,455	56,129	55,929	7.7%
#5 Black	Load at 0.01 in. Slip (lb)	Top	22,498	21,343	23,791	17,786	17,324	20,604	20,558	12.5%
		Center	22,036	22,636	26,286	24,253	23,191	23,468	23,645	6.3%
		Bottom	25,547	NA	24,715	21,759	NA	26,286	24,577	8.1%
	Max. Load (lb)	Top	26,378	25,039	26,979	23,145	21,943	22,313	24,300	8.8%
		Center	26,424	27,071	29,196	27,533	25,547	25,685	26,909	5.1%
		Bottom	30,213	NA	27,579	24,577	NA	29,889	28,065	9.3%
#8 Epoxy Coated	Load at 0.01 in. Slip (lb)	Top	35,607	46,881	45,481	52,341	52,710	47,213	46,706	13.3%
		Center	54,655	47,269	62,663	57,238	54,281	49,430	54,256	10.2%
		Bottom	53,022	54,811	60,408	NA	54,050	60,333	56,525	6.3%
	Max. Load (lb)	Top	53,172	51,001	50,031	47,036	49,446	37,396	48,014	11.6%
		Center	50,724	53,496	57,376	54,888	47,036	51,079	52,433	6.9%
		Bottom	54,466	54,928	58,624	NA	49,135	64,062	56,243	9.8%

Table A5. Pull-out test results of vertical #8 (25M) and #5 (16M) bars in CVC and SCC Slabs (PHASE III).

Concrete Type	Bar Type	Load Stage	Bar #1	Bar #2	Bar #3	Bar #4	Bar #5	Bar #6	Average (lb)	COV (%)
CVC	#8 Black	Load at 0.01 in Slip (lb)	36,264	37,650	38,620	42,547	35,525	40,422	38,505	6.8%
		Max. Load (lb)	47,398	46,197	48,737	43,009	45,227	46,335	46,151	4.2%
	#5 Black	Load at 0.01 in Slip (lb)	24,161	21,805	23,653	22,821	22,452	24,115	23,168	4.1%
		Max. Load (lb)	28,041	25,547	26,332	25,501	26,101	26,194	26,286	3.5%
	#8 Epoxy Coated	Load at 0.01 in Slip (lb)	27,395	28,781	30,628	28,827	27,395	30,998	29,004	5.3%
		Max. Load (lb)	48,229	50,863	53,080	55,898	48,645	52,803	51,586	5.7%
SCC	#8 Black	Load at 0.01 in Slip (lb)	51,833	52,526	51,694	51,509	45,688	50,585	50,639	4.9%
		Max. Load (lb)	56,129	57,145	56,545	58,624	50,077	59,086	56,268	5.8%
	#5 Black	Load at 0.01 in Slip (lb)	23,237	25,270	28,734	24,577	25,657	28,781	26,043	8.7%
		Max. Load (lb)	24,900	28,041	29,935	26,563	28,629	30,813	28,147	7.7%
	#8 Epoxy Coated	Load at 0.01 in Slip (lb)	38,944	39,129	42,362	42,732	42,547	NA	41,143	4.7%
		Max. Load (lb)	57,376	57,653	64,444	61,857	63,936	55,159	60,071	6.4%

References

- American Concrete Institute Committee 318 (ACI 318). *Building Code Requirements for Structural Concrete and Commentary*; ACI CODE 318: Farmington Hills, MI, USA, 2019.
- Mathey, R.G.; Watstein, D. Investigation of Bond in Beam and Pull-Out Specimens with High-Yield-Strength Deformed Bars. *ACI J. Proc.* **1961**, *62*, 1071–1090.
- Chan, Y.W.; Chen, Y.S.; Liu, Y.S. Development of Bond Strength of Reinforcement Steel in Self-Consolidating Concrete. *ACI Struct. J.* **2003**, *100*, 490–498.
- Hassan, A.A.A.; Hossain, K.M.A.; Lachemi, M. Bond Strength of Deformed Bars in Large Reinforced Concrete Members Cast with Industrial Self-Consolidating Concrete Mixture. *Constr. Build. Mater.* **2010**, *24*, 520–530. [[CrossRef](#)]
- Cattaneo, S.; Rosati, G. Bond between Steel and Self-Consolidating Concrete: Experiments and Modeling. *ACI Struct. J.* **2009**, *106*, 540–550.
- König, G.; Holschemacher, K.; Dehn, F.; Weibe, D. Self-compacting concrete-time development of material properties and bond behaviour. In Proceedings of the Second International RILEM Symposium on Self-Compacting Concrete, Tokyo, Japan, 11–15 December 2001; pp. 507–516.
- König, G.; Holschemacher, K.; Dehn, F.; Weibe, D. Bond of reinforcement in self-compacting concrete (SCC) under monotonic and cyclic loading. In Proceedings of the Third International RILEM Symposium on Self-Compacting Concrete, Reykjavik, Iceland, 17–20 August 2003; pp. 939–947.
- Almeida, F.M.; Nardin, S.; Gresce, A.L.H. Evaluation of the bond strength of self-compacting concrete in pull-out tests. In Proceedings of the Second North American Conference on the Design and Use of Self-Consolidating Concrete and Fourth International RILEM Symposium on Self-Compacting Concrete, Chicago, IL, USA, 26–28 May 2005; pp. 953–958.
- Almeida, F.M.; El Debs, M.K.; El Debs, A.L.H.C. Bond-Slip Behavior of Self-Compacting Concrete and Vibrated Concrete Using Pullout and Beam Tests. *Mater. Struct.* **2008**, *41*, 1073–1089.
- Aslani, F.; Nejadi, S. Bond Behavior of Reinforcement in Conventional and Self-Compacting Concrete. *Adv. Struct. Eng.* **2012**, *15*, 2033–2051. [[CrossRef](#)]
- Valcuende, M.; Parra, C. Bond Behavior of Reinforcement in Self-Compacting Concretes. *Construction and Building Materials* **2009**, *23*, 162–170. [[CrossRef](#)]
- Gibbs, J.C.; Zhu, W. Strength of Hardened Self-Compacting Concrete. In Proceedings of the 1st International Rilem Symposium on Self-Compacting Concrete, Stockholm, Sweden, 13–14 September 1999; pp. 199–209.
- Wang, G.; Zheng, J. Bond Behaviors of Self-Compacting Concrete. In Proceedings of the First International Symposium on Design, Performance and Use of Self-Consolidating Concrete, Changsha, China, 26–28 May 2005; pp. 465–471.
- Daoud, A.; Lorrain, M.; Laborderie, C. Anchorage and Cracking Behaviour of Self-Compacting Concrete. In Proceedings of the 3rd International RILEM Symposium on Self-Compacting Concrete, Bagneux, France, 17–20 August 2003; pp. 692–702.

15. Zhu, W.; Sonebi, M.; Bartos, P.J.M. Bond and interfacial properties of reinforcement in self-compacting concrete. *Mater. Struct.* **2004**, *37*, 442–448. [[CrossRef](#)]
16. Desnerck, P.; Schutter, G.D.; Taerwe, L. Bond Strength of Reinforcing Bars in Self-Compacting Concrete: Experimental Determination. In Proceedings of the 3rd North American conference on the Design and Use of Self-Consolidating Concrete, Challenges and Barriers to Application, Center for Advanced Cement-Based Materials (ACBM), Chicago, IL, USA, 10–12 November 2008; pp. 433–438.
17. Khayat, K.H. Workability, Testing, and Performance of Self-Consolidating Concrete. *ACI Mater. J.* **1999**, *96*, 346–353.
18. Attiogbe, E.K.; See, H.T.; Daczko, J.A. Engineering Properties of Self-Consolidating Concrete. In Proceedings of the First North American Conference on the Design and Use of Self-Consolidating Concrete, Chicago, IL, USA, 12–13 November 2002; pp. 331–336.
19. Castel, A.; Vidal, T.; Viriyametanon, K.; François, R. Effect of Reinforcing Bar Orientation and Location on Bond with Self-Consolidating Concrete. *ACI Struct. J.* **2006**, *103*, 559–567.
20. Trezos, K.G.; Sfikas, I.P.; Palmos, M.S.; Sotiropoulou, E.K. Top-Bar Effect in Self-Compacting Concrete Elements. Design, Production and Placement of Self-Consolidating Concrete. *RILEM Book Ser.* **2010**, *1*, 355–366.
21. Esfahani, M.R.; Lachemi, M.; Kianoush, M.R. Top-Bar Effect of Steel Bars in Self-Consolidating Concrete (SCC). *Cem. Concr. Compos.* **2008**, *30*, 52–60. [[CrossRef](#)]
22. Morcou, G.; Wang, K.; Taylor, P.; Surendra, P.S. *Self-Consolidating Concrete for Cast-in-Place Bridge Components*; National Corporative Highway Research Program (NCHRP), Project 18-16; Transportation Research Board: Washington, DC, USA, 2016.
23. Daczko, J. *Self-Consolidating Concrete: Applying What We Know*; Spon Press: New York, NY, USA, 2012.
24. European Federation of National Trade Associations (EFNARC). *The European Guidelines for Self-Compacting Concrete: Specification, Production, and Use*; EFNARC: Norfolk UK, 2005.
25. American Concrete Institute Committee 237 (ACI 237). *Self-Consolidating Concrete*; Emerging Technologies Series (ETS); ACI PRC 237R: Farmington Hills, MI, USA, 2007.
26. Khayat, K.H.; Mitchell, D. *Self-Consolidating Concrete for Precast, Prestressed Concrete Bridge Elements*; National Corporative Highway Research Program (NCHRP), Report 628; Transportation Research Board: Washington, DC, USA, 2009.
27. Precast/Prestressed Concrete Institute (PCI). *Interim Guidelines for the Use of Self-Consolidating Concrete in Precast/Prestressed Concrete Institute Member Plants*; TR-6-03; PCI: Chicago, IL, USA, 2003.
28. Domone, P. *Proportioning of Self-Compacting Concrete—The UCL Method*; Technical Report; Department of Civil, Environmental and Geomatics Engineering, University College London (UCL): London, UK, 2009.
29. European Federation of National Trade Associations (EFNARC). *Specifications and Guidelines for Self-Compacting Concrete*; EFNARC: Norfolk, UK, 2002.
30. Kheder, G.F.; Al Jadiri, R.S. New Method for Proportioning Self-Consolidating Concrete Based on Compressive Strength Requirements. *ACI Mater. J.* **2010**, *7*, 490–497.
31. Koehler, E.P.; Fowler, D.W. *ICAR Mixture Proportioning Procedure for Self-Consolidating Concrete*; ICAR Project 108-1; International Center for Aggregates Research: Austin, TX, USA, 2007.
32. Okamura, H.; Ozawa, K. Mix Design for Self-Compacting Concrete. *Concr. Libr. JSCE* **1995**, *25*, 107–120.
33. CSA CAN3-A23.3; Design of Concrete Structures; Canadian Standards Association: Rexdale, ON, Canada, 2004.
34. American Concrete Institute Committee 211 (ACI 211). *Guide for Selecting Proportions for High-Strength Concrete Using Portland Cement and Other Cementitious Materials*; ACI PRC 211.4R: Farmington Hills, MI, USA, 2008.
35. RILEM/CEB/FIP. Test and Specifications of Reinforcement for Reinforced and Pre-stressed Concrete: Four recommendations of the RILEM/CEB/FIB, 2: Pullout test. *Mater. Struct.* **1970**, *3*, 175–178.
36. CEB-fib. *Bond of Reinforcement in Concrete*; CEB-fib: Lausanne, Switzerland, 2000; Volume 10, p. 427.
37. American Concrete Institute Committee (ACI 408R). *Bond and Development of Straight Reinforcing Bars in Tension*; ACI: Farmington Hills, MI, USA, 2003.

Disclaimer/Publisher’s Note: The statements, opinions and data contained in all publications are solely those of the individual author(s) and contributor(s) and not of MDPI and/or the editor(s). MDPI and/or the editor(s) disclaim responsibility for any injury to people or property resulting from any ideas, methods, instructions or products referred to in the content.